

University of Groningen

## The geographic distribution of bioavailable strontium isotopes in Greece – A base for provenance studies in archaeology

Frank, Anja B.; Frei, Robert; Moutafi, Ioanna; Voutsaki, Sofia; Orgeolet, Raphaël; Kristiansen, Kristian; Frei, Karin M.

*Published in:*  
Science of the Total Environment

*DOI:*  
[10.1016/j.scitotenv.2021.148156](https://doi.org/10.1016/j.scitotenv.2021.148156)

**IMPORTANT NOTE: You are advised to consult the publisher's version (publisher's PDF) if you wish to cite from it. Please check the document version below.**

*Document Version*  
Publisher's PDF, also known as Version of record

*Publication date:*  
2021

[Link to publication in University of Groningen/UMCG research database](#)

### *Citation for published version (APA):*

Frank, A. B., Frei, R., Moutafi, I., Voutsaki, S., Orgeolet, R., Kristiansen, K., & Frei, K. M. (2021). The geographic distribution of bioavailable strontium isotopes in Greece – A base for provenance studies in archaeology. *Science of the Total Environment*, 791, Article 148156. <https://doi.org/10.1016/j.scitotenv.2021.148156>

### **Copyright**

Other than for strictly personal use, it is not permitted to download or to forward/distribute the text or part of it without the consent of the author(s) and/or copyright holder(s), unless the work is under an open content license (like Creative Commons).

The publication may also be distributed here under the terms of Article 25fa of the Dutch Copyright Act, indicated by the "Taverne" license. More information can be found on the University of Groningen website: <https://www.rug.nl/library/open-access/self-archiving-pure/taverne-amendment>.

### **Take-down policy**

If you believe that this document breaches copyright please contact us providing details, and we will remove access to the work immediately and investigate your claim.

Downloaded from the University of Groningen/UMCG research database (Pure): <http://www.rug.nl/research/portal>. For technical reasons the number of authors shown on this cover page is limited to 10 maximum.



## The geographic distribution of bioavailable strontium isotopes in Greece – A base for provenance studies in archaeology



Anja B. Frank<sup>a,\*</sup>, Robert Frei<sup>b</sup>, Ioanna Moutafi<sup>c,d</sup>, Sofia Voutsaki<sup>e</sup>, Raphaël Orgeolet<sup>f,g</sup>, Kristian Kristiansen<sup>h</sup>, Karin M. Frei<sup>a</sup>

<sup>a</sup> Department of Research, Collections and Conservation, Environmental Archaeology and Materials Science, National Museum of Denmark, Kongens Lyngby DK 2800, Denmark

<sup>b</sup> Department of Geosciences and Natural Resource Management, University of Copenhagen, DK, 1350 Copenhagen, Denmark

<sup>c</sup> McDonald Institute for Archaeological Research, University of Cambridge, UK, CB2 3ER Cambridge, United Kingdom

<sup>d</sup> The M.H. Wiener Laboratory for Archaeological Science, American School of Classical Studies at Athens, Souidias 54, 10676 Athens, Greece

<sup>e</sup> Groningen Institute of Archaeology, University of Groningen, NL-9712, ER Groningen, Netherlands

<sup>f</sup> Aix Marseille Université, CNRS, Centre Camille Jullian, Aix-en-Provence, France

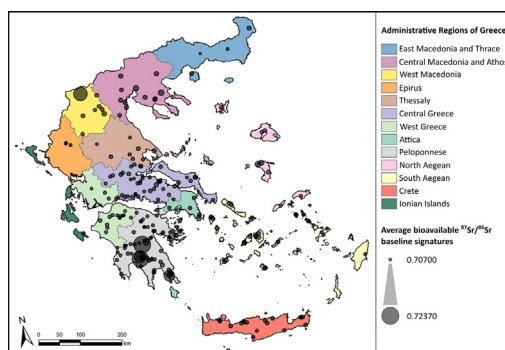
<sup>g</sup> École française d'Athènes, Athens, Greece

<sup>h</sup> Department of Historical Studies, University of Gothenburg, SE, 41255 Gothenburg, Sweden

### HIGHLIGHTS

- We present bioavailable Sr data from plants, soils and waters from Central Greece.
- Carbonate weathering appears to control the Sr isotope signatures of the proxies.
- The applicability of the environmental proxies as baseline material is evaluated.
- Statistical, bioavailable  $^{87}\text{Sr}/^{86}\text{Sr}$  ranges are defined for Greece and its provinces.
- These can serve as reference baselines in human mobility studies.

### GRAPHICAL ABSTRACT



### ARTICLE INFO

#### Article history:

Received 12 March 2021

Received in revised form 4 May 2021

Accepted 27 May 2021

Available online 4 June 2021

Editor: Xinbin Feng

#### Keywords:

Strontium isotopes

$^{87}\text{Sr}/^{86}\text{Sr}$  baseline

Mobility studies

Archaeology

Multi-proxy comparison

Greece

### ABSTRACT

Sr isotopes are a powerful tool used to reconstruct human mobility in archaeology. This requires extensive bioavailable  $^{87}\text{Sr}/^{86}\text{Sr}$  baselines used as reference for deciphering potential areas of origin. We define the first extensive bioavailable Sr isotope baselines for the different geographical regions and surface lithologies of Greece by combining new Sr data with previously published bioavailable  $^{87}\text{Sr}/^{86}\text{Sr}$  data. We present 82 new Sr concentrations and  $^{87}\text{Sr}/^{86}\text{Sr}$  signatures of plants, soil leachates, surface waters and spring waters from Central Greece and combine these with published baseline values from all over Greece. We define individual baselines for ten of the thirteen geographical regions of Greece. We also provide soil leachate  $^{87}\text{Sr}/^{86}\text{Sr}$  ratios from the two archaeological Bronze Age sites of Kirrha and Ayios Vasileios in Central and Southern Greece and demonstrate the validity and applicability of the new baselines for these sites. The bioavailable  $^{87}\text{Sr}/^{86}\text{Sr}$  compositions of Central Greece define a narrow range of  $^{87}\text{Sr}/^{86}\text{Sr}$  values between 0.70768 – 0.71021, with the widest range observed for the soil leachates. Sr derived from carbonate weathering appears to be the most important Sr source sampled by the proxies. There is an overall larger variability in baseline ranges of the different geographical regions, the narrowest is that for West Greece and the widest that for West Macedonia. In addition, we computed statistical Sr isotope ranges for the five main surface lithological groups characterising the sampling sites of the various proxies. Narrowly ranged, unradiogenic bioavailable Sr isotope signatures are typical of areas characterised by igneous outcrops

\* Corresponding author.

E-mail addresses: [anja.frank@natmus.dk](mailto:anja.frank@natmus.dk) (A.B. Frank), [robertf@ign.ku.dk](mailto:robertf@ign.ku.dk) (R. Frei), [s.voutsaki@rug.nl](mailto:s.voutsaki@rug.nl) (S. Voutsaki), [kristian.kristiansen@archaeology.gu.se](mailto:kristian.kristiansen@archaeology.gu.se) (K. Kristiansen), [Karin.M.Frei@natmus.dk](mailto:Karin.M.Frei@natmus.dk) (K.M. Frei).

as well as by Cenozoic and Mesozoic sediments. Areas, where Palaeozoic and Precambrian bedrock outcrops dominate, produce significantly wider ranges. Our study promotes the usefulness of multi-proxy baselines for geographical reference purposes and thus their promising applicability for future human mobility studies.

© 2021 Elsevier B.V. All rights reserved.

## 1. Introduction

Sr isotopes have been established in archaeology as a powerful tracing tool of past human mobility (e.g. Bentley, 2006; Frei et al., 2015; Montgomery, 2010). The radioactive decay of  $^{87}\text{Rb}$  to  $^{87}\text{Sr}$  results in a large range in the ratio of radiogenic strontium-87 ( $^{87}\text{Sr}$ ) and stable strontium-86 ( $^{86}\text{Sr}$ ) in Earth's surface environment (e.g. Capo et al., 1998; Tommasini et al., 2018). This range can be utilised as a base for provenancing human remains, by comparing their respective  $^{87}\text{Sr}/^{86}\text{Sr}$  values with the  $^{87}\text{Sr}/^{86}\text{Sr}$  background of the area they were unearthed from or are suspected to originate from.

Sr is released into the surface environment via weathering of bedrock and soils and is taken up by plants from pore waters, surface runoff and groundwater (Bentley, 2006; Price et al., 2002). Humans ingest Sr via their diet, sourcing most of their Sr from drinking water and plant-based foods (Coelho et al., 2017; Rose et al., 2010), and fix it within their skeleton where it replaces calcium (Bentley, 2006; Montgomery, 2010).  $^{87}\text{Sr}/^{86}\text{Sr}$  ratios do not fractionate significantly along that pathway (Flockhart et al., 2015), allowing a direct comparison between human  $^{87}\text{Sr}/^{86}\text{Sr}$  values and the proportion of Sr accessible for uptake by flora and fauna (bioavailable Sr) in suspected areas of origin to trace individual mobility.

In recent years, there has been an increase in  $^{87}\text{Sr}/^{86}\text{Sr}$  data across many parts of Europe, including Greece, defining the ranges in  $^{87}\text{Sr}/^{86}\text{Sr}$  composition characteristic for these areas (Sr isotope baseline). However, to date no comprehensive bioavailable Sr isotope baselines exist for Greece as a whole, as most studies defining bioavailable  $^{87}\text{Sr}/^{86}\text{Sr}$  baselines focus on single sites or contexts. This results in a spotty geographical coverage, in particular in central and northern Greece. Further, no consensus exists on how to establish a reliable  $^{87}\text{Sr}/^{86}\text{Sr}$  isotope baseline for human mobility studies (Grimstead et al., 2017). Bioavailable Sr in the surface environment of a given target area is sourced from a range of endogenous and exogenous sources. Endogenous Sr is generally sourced from the weathering of minerals within bedrock and soils. The occurrence of a variety of minerals with drastically different Rb/Sr ratios and with variable formation ages, in combination with significantly different susceptibilities towards weathering, impart a complex release pattern of rock and soil hosted Sr to the mobile strontium fractions which are readily bioavailable (Bentley, 2006; Capo et al., 1998). Exogenous Sr sources include dry and wet atmospheric depositions as well as anthropogenic contamination, which can add a foreign Sr signal to a surface environment (Bentley, 2006; Frei and Frei, 2013). Hence, a wide range in proxies has been used to best mimic and characterise bioavailable Sr fractions and their respective isotopic compositions, to define bioavailable  $^{87}\text{Sr}/^{86}\text{Sr}$  reference baselines in Greece. These include modern environmental samples (e.g. Frank et al., 2021; Vaiglova et al., 2018), faunal remains (e.g. Nafplioti, 2011; Whelton et al., 2018) and human archaeological bones (e.g. Nafplioti, 2011; Triantaphyllou et al., 2015). The choice of proxy is usually tailored to the aim of the study, and is often limited by the availability of respective proxy materials.

In the present study we present  $^{87}\text{Sr}/^{86}\text{Sr}$  values and Sr concentrations for different modern environmental proxies (plants, soils, surface waters and spring waters) from Central Greece and for the cultural layers of two Bronze Age sites from central and southern Greece (Kirrha and Ayios Vasileios). The aim of the study is to contribute to our understanding of modern environmental proxies and their usefulness for characterising bioavailable Sr isotope signatures that can serve to constrain the distribution of bioavailable  $^{87}\text{Sr}/^{86}\text{Sr}$  in Greece. We therefore

address two issues: 1) We contribute to the discussion centred around proxy suitability by presenting  $^{87}\text{Sr}/^{86}\text{Sr}$  values from different environmental proxies from Central Greece. In doing this, we also fill in the gap in bioavailable  $^{87}\text{Sr}/^{86}\text{Sr}$  data in this region. 2) We define the first extensive bioavailable Sr isotope baselines for the different geographical regions and surface lithologies of Greece by combining our Sr data with previously published bioavailable  $^{87}\text{Sr}/^{86}\text{Sr}$  data and evaluate them through comparison with the  $^{87}\text{Sr}/^{86}\text{Sr}$  data from the cultural layers of Kirrha and Ayios Vasileios.

## 2. Background

### 2.1. Geology of Greece

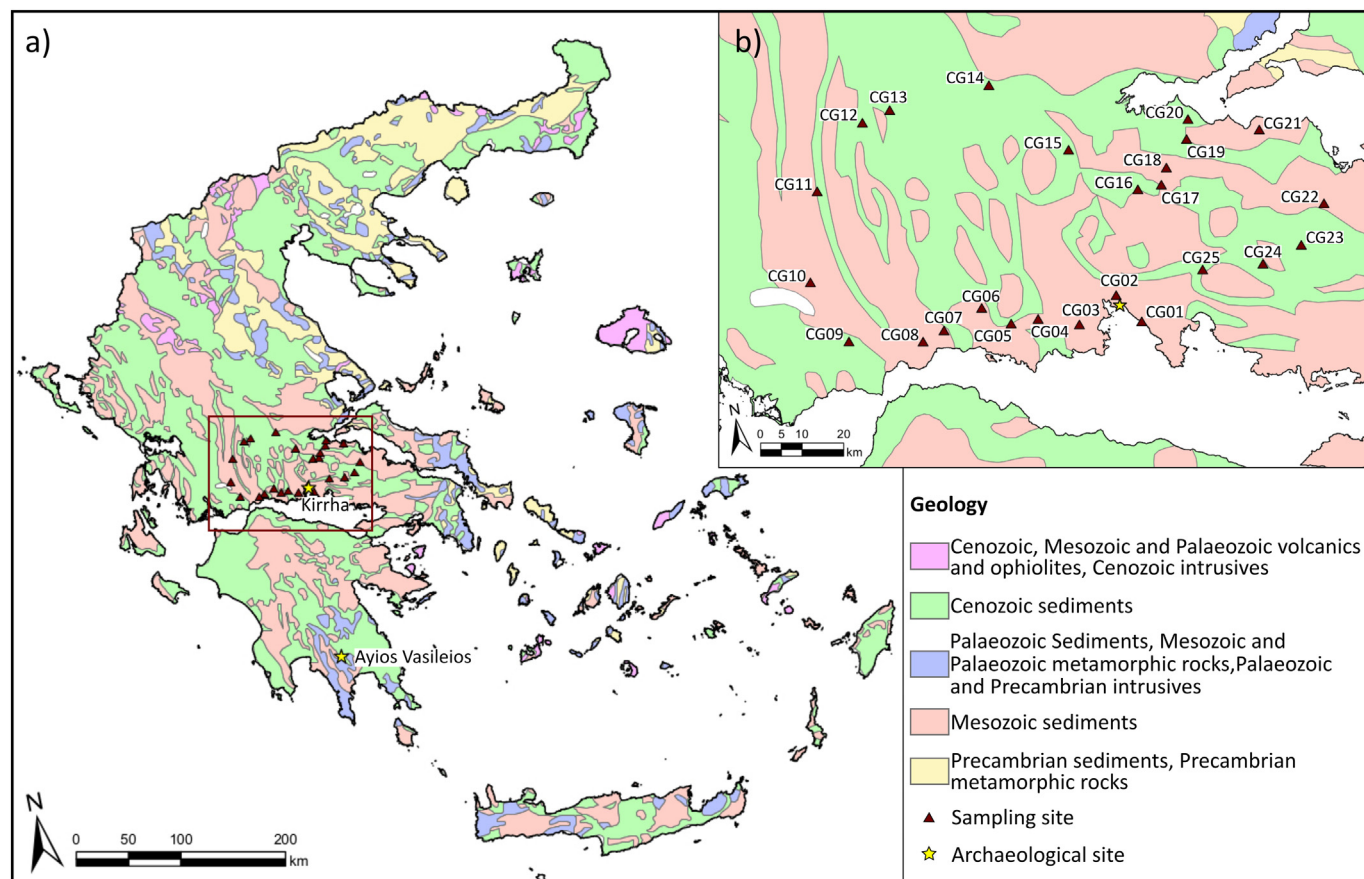
As a result of strong tectono-metamorphic and orogenic activity, Greece is characterised by a complex relief and geology. Large parts of the country are mountainous with notable mountain ranges, such as the Rhodope mountain range, which forms the border between Greece and Bulgaria, and the Pindos mountain range, which stretches from the northwest of the country to the southeast extending across the Peloponnese and many Aegean islands, such as Crete. The geology of Greece is divided into distinct geotectonic units comprised of nine tectono-stratigraphic terranes (Papanikolaou, 2013, 2015). However, in many parts of the country these units are not always lithologically reflected by the respective outcrop patterns of the rocks pertaining to these units as they are covered by post-Alpine, mainly Quaternary, erosional sediment deposits.

Fig. 1 shows a simplified geological map of Greece, which assembles the different surface lithologies found in Greece into five groups: 1) The Cenozoic, Mesozoic and Palaeozoic volcanic rocks, ophiolites and Cenozoic intrusives (referred to as 'igneous outcrops' in the following); 2) the Cenozoic sediments; 3) the Palaeozoic sediments, Mesozoic and Palaeozoic metamorphic rocks and Palaeozoic and Precambrian intrusives (referred to as 'Palaeozoic outcrops' in the following); 4) the Mesozoic sediments; and 5) the Precambrian sediments and Precambrian metamorphic rocks groups (referred to as 'Precambrian outcrops' in the following). Most of Greece is covered by Cenozoic and Mesozoic sediments. The Cenozoic sediments are mainly clastic sediments, such as flysch and conglomerates, while the Mesozoic sediments are predominantly carbonates (BGR, 2020; EGD, 2019). The northeast of Greece is characterised by extensive Palaeozoic and Precambrian rock outcrops, which also extend south east into the Peloponnese and the Aegean islands. The most common outcrops found within these areas are dominated by phyllites, shists and gneisses (BGR, 2020; EGD, 2019). Igneous outcrops are mainly found on the Aegean islands and in the north of Greece and are dominated by a range of plutonic and volcanic rocks (BGR, 2020).

The study area in Central Greece is dominated by Cenozoic and Mesozoic sediments (Fig. 1). These are commonly flysch sediments and limestones, respectively (BGR, 2020). Further, small ophiolite complexes are found within the north of the study area (BGR, 2020; EGD, 2019).

### 2.2. Available $^{87}\text{Sr}/^{86}\text{Sr}$ baseline data for Greece

Most studies utilising Sr isotopes in Greece focused on defining the local Sr isotope baseline of a limited target area, resulting in an uneven coverage with many parts of the country, in particular northern and central Greece, underrepresented (Fig. 2). This study partially remedies



**Fig. 1.** Locations of the sampling sites and archaeological sites investigated in this study over a simplified surface lithology map of Greece (a) and our study area (b). The surface lithology map was based on a simplified version of Pawlewicz et al. (1997) published by Voerkelius et al. (2010).

this by adding 25 additional sample sites to the centre of mainland Greece. The methods used to procure  $^{87}\text{Sr}/^{86}\text{Sr}$  baseline data varied significantly depending on the aim of the respective studies. Provenance studies of objects or building materials, such as glass or marble, generally use bulk rock  $^{87}\text{Sr}/^{86}\text{Sr}$  values to characterise the signature range of a suspected area of origin. Human mobility studies on the other hand rely on the bioavailable  $^{87}\text{Sr}/^{86}\text{Sr}$  fraction characterising a suspected target area, which can differ considerably from the areas bulk  $^{87}\text{Sr}/^{86}\text{Sr}$  signature. The bioavailable signature can be determined using a range of materials, such as modern and archaeological animal remains, or modern environmental archives. In the following paragraphs we give an overview over the available  $^{87}\text{Sr}/^{86}\text{Sr}$  data for Greece.

### 2.2.1. Archaeological mobility studies

Despite the long and rich history of Greece, only a handful of archaeological mobility studies utilising bioavailable Sr isotopes have been conducted for Greece thus far, with most of them focusing on a single context with a limited geographical range. The geographically most extensive archaeological study was conducted by Prevedorou (2015), who presented bioavailable  $^{87}\text{Sr}/^{86}\text{Sr}$  data for 42 different locations, most of which were located on the Aegean islands and the eastern mainland. The study used modern proxies (water, snail shells and faunal remains) reporting a total range in  $^{87}\text{Sr}/^{86}\text{Sr}$  ratios of 0.70684 to 0.71068. Another geographically extensive study was conducted by Nafplioti (2011; and references therein) and focused mainly on the Aegean, but also some parts of the Greek mainland and Crete. The study determined the compositional range of bioavailable  $^{87}\text{Sr}/^{86}\text{Sr}$  ratios using archaeological and modern animal skeletal tissue (e.g. snail shells or pig teeth) and archaeological human bone and recorded for 26 sampling sites a total range in bioavailable  $^{87}\text{Sr}/^{86}\text{Sr}$  ratios from 0.78154 to 0.71187. Additionally,  $^{87}\text{Sr}/^{86}\text{Sr}$  data of archaeological human bone and dentine is available for

two Bronze Age archaeological sites in western Crete (Kephala Petras and Livari-Skiadi), which suggest a narrow bioavailable range with  $^{87}\text{Sr}/^{86}\text{Sr}$  values from 0.70878 to 0.70907 (Triantaphyllou et al., 2015). On the Peloponnese, a study on Neanderthal humanoid mobility returned  $^{87}\text{Sr}/^{86}\text{Sr}$  values between 0.7086 and 0.7094 for animal dentine found in Lakonis Cave (Richards et al., 2008) and the range in bioavailable  $^{87}\text{Sr}/^{86}\text{Sr}$  values around the ancient city of Stymphalos was constrained as 0.7075 to 0.71012 using the teeth of archaeological sheep/goats and pigs (Leslie, 2012). For the prehistoric Sarakenos Cave in Central Greece, a range in bioavailable  $^{87}\text{Sr}/^{86}\text{Sr}$  values from 0.70820 to 0.70926 was determined using local plant samples (Wang et al., 2019). In a study on mobility during the Iron Age, a range in bioavailable  $^{87}\text{Sr}/^{86}\text{Sr}$  between 0.7078 and 0.7103 was reported for three archaeological sites in south-eastern Thessaly based on modern snail shells and plant samples (Panagiotopoulou et al., 2018). In another study on animal husbandry practices, measurements of modern animal remains and plants along the southern border of Thessaly returned  $^{87}\text{Sr}/^{86}\text{Sr}$  values between 0.70812 and 0.70938 (Bishop et al., 2020). Finally, Whelton et al. (2018) and Vaiglova et al. (2018) investigated seven archaeological settlements in south-western Macedonia constraining the range of bioavailable Sr isotope compositions of the area to values between 0.70822 and 0.71148 using faunal teeth and vegetation samples.

### 2.2.2. Other published $^{87}\text{Sr}/^{86}\text{Sr}$ data

Due to the versatile application of bioavailable Sr isotopes as a provenance tool in food authenticity studies, as well as in archaeological and forensic sciences, recent investigations have increasingly focussed on defining large scale regional baselines over case specific local baselines. These studies provide additional bioavailable  $^{87}\text{Sr}/^{86}\text{Sr}$  data, also for Greece. In a recent study, plant, water and soil leachate  $^{87}\text{Sr}/^{86}\text{Sr}$  data from 52 sites across the Peloponnese peninsula were presented, and

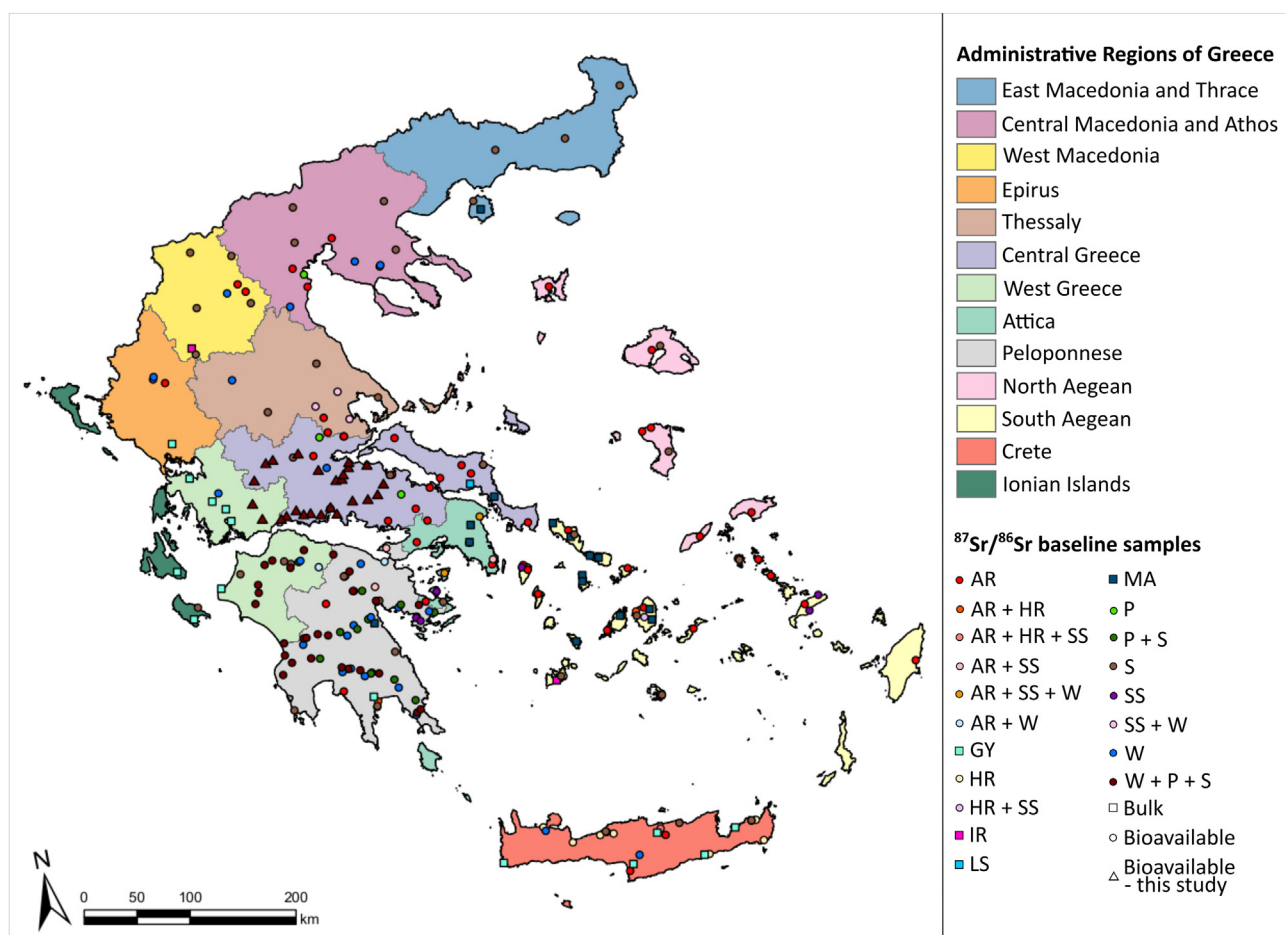


**Fig. 2.** Map of published  $^{87}\text{Sr}/^{86}\text{Sr}$  data for the different regions of Greece (Barton et al., 1983; Bishop et al., 2020; Brilli et al., 2005; Frank et al., 2021; Gale et al., 1988; Gärtner et al., 2011; Hoogewerff et al., 2019; Leslie, 2012; Nafplioti, 2008, 2011; Panagiotopoulou et al., 2018; Prevedorou, 2015; Tremba et al., 1975; Triantaphyllou et al., 2015; Vaiglova et al., 2018; Valsami-Jones and Cann, 1994; Voerkelius et al., 2010; Wang et al., 2019; Whelton et al., 2018). Bioavailable  $^{87}\text{Sr}/^{86}\text{Sr}$  data (circles and triangles) was determined using animal remains (AR), human remains (HR), plants (P), soils (S), snail shells (SS) and water (W). Bulk  $^{87}\text{Sr}/^{86}\text{Sr}$  data (squares) was reported for gypsum (GY), igneous rocks (IR), limestone (LS) and marble (MA).

these data define a total range in bioavailable  $^{87}\text{Sr}/^{86}\text{Sr}$  values between 0.70779 and 0.72370 (Frank et al., 2021). Soil leachate data is also available from a Europe-wide study investigating grazing and agricultural soils conducted by Hoogewerff et al. (2019). These authors reported bioavailable  $^{87}\text{Sr}/^{86}\text{Sr}$  values between 0.70710 and 0.71992 for 46 soils across Greece. Finally, Voerkelius et al. (2010) analysed spring waters from across Europe, including 13 from Greece. Data in this particular study define a  $^{87}\text{Sr}/^{86}\text{Sr}$  value range from 0.70782 to 0.70946.

Fig. 2 also includes bulk rock  $^{87}\text{Sr}/^{86}\text{Sr}$  data from geochemical and material provenance studies conducted in Greece. Bulk  $^{87}\text{Sr}/^{86}\text{Sr}$  values of the bedrock of an area are commonly inadequate to trace biological material (e.g. Bentley, 2006). However, as weathering of the bedrocks is generally a major source contributing to the bioavailable Sr composition of an area (e.g. Bentley, 2006; Montgomery, 2010), bulk rock  $^{87}\text{Sr}/^{86}\text{Sr}$  data can give valuable insight into the regional source end-members. Therefore, we included such data sets herein. Most bulk rock  $^{87}\text{Sr}/^{86}\text{Sr}$  signatures reported for Greece were conducted to constrain the provenance of building materials. To provenance gypsum, Gale et al. (1988) investigated gypsum deposits from Crete, the Peloponnese and western Greece, whose average  $^{87}\text{Sr}/^{86}\text{Sr}$  composition range between 0.70752 and 0.70886. Marble quarries from the Aegean islands, the Peloponnese and Attica are characterised by average  $^{87}\text{Sr}/^{86}\text{Sr}$  compositions between 0.70710 and 0.70822 (Brilli et al., 2005; Gärtner et al., 2011). For Euboea, a geochemical study further reported average marble and limestone  $^{87}\text{Sr}/^{86}\text{Sr}$  compositions of 0.70776 and 0.70734, respectively (Tremba et al., 1975). The average  $^{87}\text{Sr}/^{86}\text{Sr}$  signatures of calc-alkaline lavas on the islands of Santorini and Milos

were determined as 0.70504 and 0.70600, respectively (Barton et al., 1983), and hydrothermally altered basaltic rocks of the Pindos ophiolites yielded an average  $^{87}\text{Sr}/^{86}\text{Sr}$  composition of 0.70534 as determined by Valsami-Jones and Cann (1994).

### 2.3. Archaeological sites

The archaeological sites of Kirrha and Ayios Vasileios are two Bronze Age settlements in Greece (Fig. 1). Both sites are of special significance to the understanding of social dynamics in the so called “transitional” period from Middle to Late Bronze Age on the Greek mainland. The changing burial customs observed in both sites reflect a vibrant discourse between the past, present and future, well in accordance with the changing social landscape of this seminal period at the dawn of the Mycenaean civilization (Lagia et al., 2016; Moutafi and Voutsaki, 2016). Hence, Kirrha and Ayios Vasileios are ideal sites to investigate the connection between individual mobility and changing traditions and were thus included to evaluate the applicability of the baselines calculated for Greece herein for future mobility studies. A detailed description of both sites is given in Supplement S1.

## 3. Material and methods

### 3.1. Material and sampling

A total of 82 environmental samples (water, plants and soils) were collected from 25 sites across Central Greece to constrain bioavailable

**Table 1**  
 $^{87}\text{Sr}/^{86}\text{Sr}$  value, its double standard error (2SE) and Sr concentration measured for plant, soil leachate, surface water and spring water samples at 25 locations in Central Greece with Mesozoic- or Cenozoic-aged sediments.

Location	Surface lithology	Plants			Soil leachates			Surface waters			Spring waters			Distance to location (km)
		$^{87}\text{Sr}/^{86}\text{Sr}$	2SE	Sr (mg/kg)	$^{87}\text{Sr}/^{86}\text{Sr}$	2SE	Sr (mg/kg)	$^{87}\text{Sr}/^{86}\text{Sr}$	2SE	Sr (mg/l)	$^{87}\text{Sr}/^{86}\text{Sr}$	2SE	Sr (mg/l)	
CG01	Mesozoic sediments	0.709106	0.000016	2.50	0.708718	0.000021	7.19				0.708468	0.000018	0.08	1.44
CG02	Mesozoic sediments	0.708176	0.000016	7.73	0.708107	0.000019	10.52				0.708465	0.000016	0.21	1.8
CG03	Mesozoic sediments	0.708706	0.000016	4.83	0.708225	0.000019	6.03				0.708097	0.000020	0.06	3.24
CG04	Mesozoic sediments	0.708380	0.000008	110.43	0.708386	0.000023	19.36				0.708406	0.000020	0.09	1.19
CG05	Mesozoic sediments	0.708955	0.000009	16.12	0.708795	0.000018	15.06	0.708893	0.000020	0.56				
CG06	Mesozoic sediments	0.708880	0.000021	10.94	0.708864	0.000019	11.23	0.708580	0.000020	0.18	0.708505	0.000021	0.21	3.07
CG07	Mesozoic sediments	0.708014	0.000009	22.09	0.707953	0.000019	23.67				0.708349	0.000017	0.29	1.03
CG08	Mesozoic sediments	0.708284	0.000020	6.99	0.708064	0.000021	7.97	0.708061	0.000018	0.39	0.708131	0.000018	0.43	3.64
CG09	Cenozoic sediments	0.708255	0.000014	25.33	0.708549	0.000018	13.91	0.707973	0.000019	0.29	0.708341	0.000022	0.64	2.04
CG10	Mesozoic sediments	0.708398	0.000016	13.35	0.708889	0.000019	19.99	0.707842	0.000019	0.29				
CG11	Cenozoic sediments	0.708229	0.000021	20.21	0.708369	0.000021	8.11	0.708148	0.000015	0.28				
CG12	Cenozoic sediments	0.708349	0.000018	14.08	0.708245	0.000020	10.32				0.708460	0.000017	0.33	6.98
CG13	Cenozoic sediments	0.708833	0.000017	26.23	0.708814	0.000021	11.23				0.708325	0.000023	0.17	0.51
CG14	Cenozoic sediments	0.709099	0.000020	12.49	0.709448	0.000016	19.36	0.708025	0.000016	0.29	0.709055	0.000020	0.51	0.95
CG15	Cenozoic sediments	0.707702	0.000011	24.93	0.707675	0.000017	34.36				0.708907	0.000022	0.31	3.19
CG16	Cenozoic sediments	0.708975	0.000011	7.64	0.709449	0.000019	10.72	0.707923	0.000021	0.06				
CG17	Mesozoic sediments	0.708636	0.000020	4.16	0.708900	0.000015	5.88	0.708057	0.000015	0.06				
CG18	Mesozoic sediments	0.707927	0.000021	2.47	0.707857	0.000020	5.04	0.708261	0.000018	0.07	0.708239	0.000010	0.08	0
CG19	Cenozoic sediments	0.708284	0.000017	6.16	0.708208	0.000021	4.27	0.708221	0.000018	0.21	0.708181	0.000014	0.23	0
CG20	Cenozoic sediments	0.708232	0.000019	6.08	0.707783	0.000020	4.32	0.708144	0.000021	0.10				
CG21	Mesozoic sediments	0.708491	0.000018	8.69	0.708380	0.000022	4.89	0.708404	0.000015	0.13				
CG22	Mesozoic sediments	0.710160	0.000017	3.37	0.710212	0.000024	3.63	0.709949	0.000013	0.19	0.708145	0.000017	0.14	6.33
CG23	Cenozoic sediments	0.708944	0.000019	4.25	0.708626	0.000021	8.62	0.708221	0.000016	0.10				
CG24	Cenozoic sediments	0.709733	0.000013	4.68	0.709191	0.000016	9.03				0.708186	0.000021	0.09	5.6
CG25	Cenozoic sediments	0.708468	0.000018	4.21	0.707961	0.000021	10.64				0.707685	0.000022	0.05	6.42

Sr isotope ranges of an otherwise largely unexplored area of Greece's mainland (Table 1). The sites were distributed evenly between the Cenozoic (12 sites) and Mesozoic sediments (13 sites) encompassing the study areas' surface lithology. Wherever possible, pristine, unfarmed locations were preferred. Our site classification into 'natural' and 'agricultural' is based on the land use of the sites' immediate surroundings (Supplement S2). Natural sites refer to pristine, undisturbed locations, such as forests or national parks and were commonly found in mountainous terrane. The agricultural sites refer to orchards, pastures and grasslands, while crop fields were excluded due to the intense fertiliser use common for such fields. Agricultural areas usually dominated the flat terranes, plains and river valleys.

For logistical purposes, sites from which all three proxies (water, plants and soils) could be sampled within a ~250 m radius were preferred. Water was preferably sampled from running surface water bodies (river and streams). In dry areas where no significant surface water was present, spring water was collected instead from local fountains located up to 7 km from the sampling sites to supplement our dataset. To determine a site's average bioavailable Sr isotope composition, three soils and plants were sampled within a ~250 m radius at each location. Soil samples correspond to topsoils taken 5–10 cm below the soil surface. The depth was chosen to avoid the organic surface layer. For the plant samples, shrubs or small trees within close proximity of the soil locations were chosen. Plants of up to 3 m in height were sampled to ensure a root system that samples large parts of the soil profile, but is minimal influenced by the organic surface layer or deep groundwater. The sampled species depended on the availability and included inter alia sage, maple and olive (Supplement S2). Leaves were taken from different heights of the shrubs to ensure a homogenised, representative sample.

Besides the modern environmental samples, soil samples were taken from the cultural layers of Kirrha and Ayios Vasileios. Care was taken to choose samples from different areas of the two cemeteries and from different types of graves. The samples were always taken rather deep in the grave, and collected at the stratigraphic level of the

skeletons, around or inside bones. A more detailed description of the sampled graves is given in Supplement S3.

### 3.2. Sample preparation

To remove any particulate matter, the water samples were filtered using 0.45  $\mu\text{m}$  syringe filters. From each sample, 5 ml were pipetted into pre-cleaned Teflon beakers. The aliquots were spiked with a  $^{84}\text{Sr}$  enriched tracer to determine the Sr concentration via isotope dilution (ID) and subsequently dried down on a hot plate at 100 °C overnight.

The sampled leaves were cleaned with moist KIMTECH wipes to remove any dust and were then air-dried. The air-dried samples were subsequently crushed using an agate mortar. For every sample site, a composite plant sample consisting of ~33 mg plant material from each of its three subsamples (resulting in ~100 mg combined plant material from the site) were weighed into pre-cleaned ceramic crucibles. The samples were placed in a laboratory muffle furnace and incinerated at 750 °C for 5 h. Once cooled, the samples were transferred with ~2 ml ultra-clean (Milli-Q 18M $\Omega$  resistivity) water (MQ) into pre-cleaned Teflon beakers. Next, the samples were dried down on a hot plate at 100 °C before being further digested using 1 ml concentrated HNO<sub>3</sub>. After being dried down again, the samples were re-dissolved in 2 ml 3 M HNO<sub>3</sub> and placed into an ultrasonic bath for ~10 min. Finally, 1 ml aliquots were removed from the samples, spiked with an adequate amount of  $^{84}\text{Sr}$  enriched tracer, and dried down again.

The air-dried modern soil samples were carefully ground using an agate mortar. For the preparation of composite leachates of modern soil samples, 0.33 g of each of the three subsamples taken at one site were weighed into a 15 ml test tube, which amounted to a total soil sample amount of ~1 g. The archaeological soil samples were sieved and ground. For the leachates, 1 g of soil from each of the cultural layer samples was weighed into 15 ml test tubes. The samples were then reacted with 5 ml of a 1 M ammonium nitrate (NH<sub>4</sub>NO<sub>3</sub>) solution in an overhead-shaker for 2 h and left to settle for 1 h. Next, the samples

**Table 2**

$^{87}\text{Sr}/^{86}\text{Sr}$  value, its double standard error (2SE) and Sr concentration measured for eleven archaeological soils sampling the cultural layers of Kirrha and Ayios Vasileios.

Sample ID	Specifics	$^{87}\text{Sr}/^{86}\text{Sr}$	2SE	Sr (mg/kg)
<b>Ayios Vasileios</b>				
AV01	Grave 13	0.708812	0.000023	2.33
AV02	Grave 17	0.708853	0.000017	2.92
AV03	Grave23	0.708639	0.000019	4.28
AV04	Burial 25	0.709011	0.000025	3.19
<b>Kirrha</b>				
K01	Locus 101	0.708526	0.000019	14.78
K02	Locus 515	0.708532	0.000015	15.15
K03	Locus 567	0.708586	0.000008	14.48
K04	Locus 790	0.708559	0.000017	13.48
K05	Locus 802	0.708536	0.000023	15.69
K06	Locus 1269.7	0.708582	0.000018	16.60
K07	Locus 3311.S.1	0.708481	0.000019	15.87

were centrifuged and 0.5 ml aliquots were pipetted into pre-cleaned Teflon beakers. The aliquots were spiked with a  $^{84}\text{Sr}$  enriched tracer and dried down on a hot plate at 100 °C. This extraction procedure follows in large parts the methods applied in the Europe-wide soil-based bioavailable strontium isotope survey, which was performed as part of the Geochemical Mapping of Agricultural and Grazing Land Soil (GEMAS) framework program (Hoogewerff et al., 2019).

### 3.3. Sr separation and thermal ionisation mass spectrometry (TIMS)

The Sr separation procedure followed in large parts the method introduced by Frei and Frei (2011). 1 ml pipette tips were mounted with pressed-in filters that were pre-cleaned in 6 M HCl to be used as disposable extraction columns. The columns were charged with 200 µl pre-cleaned SrSpec™ resin (50–100 mesh; Eichrome Inc./Tristchem) and conditioned with 3 M HNO<sub>3</sub>. The dried down water, soil leachate and plant residues were re-dissolved in a few drops of 3 M HNO<sub>3</sub> and loaded onto the columns. To separate Sr, the column matrices were rinsed with ~10 ml 3 M HNO<sub>3</sub> before Sr could be collected using ~2 ml MQ. The collected solutions were dried down on a hot plate at 120 °C overnight. Finally, the samples were loaded onto previously outgassed 99.98% single Re filaments using 2.5 µl of a Ta<sub>2</sub>O<sub>5</sub>-H<sub>3</sub>PO<sub>4</sub>-HF activator solution to prepare them for TIMS measurements.

The Sr isotopic compositions and concentrations were determined at the Department of Geoscience and Natural Resource Management (IGN) at the University of Copenhagen using a VG Sector 54 IT mass spectrometer equipped with eight Faraday detectors. The samples were analysed in dynamic multi-collector runs with analysing intensities  $\geq 1$  V for  $^{88}\text{Sr}$  and analysing temperatures between 1300 and 1350 °C. Repeated analyses of loads of SRM 987 Sr standard yielded a  $^{87}\text{Sr}/^{86}\text{Sr}$  ratio of  $0.710238 \pm 0.000020$  ( $n = 7, 2\sigma$ ), which is slightly lower than the published value for SRM 987 of 0.710245 (Thirlwall, 1991). The measured sample  $^{87}\text{Sr}/^{86}\text{Sr}$  values were corrected for this offset. Recorded within-run precisions (2SE) of individual runs were consistently  $<0.0025\%$  (Tables 1+2). Procedural Sr blank amounts were generally  $<60$  pg and blank  $^{87}\text{Sr}/^{86}\text{Sr}$  values varied between 0.7095 and 0.7122. These blank Sr contributions are insignificant when considering the large amounts of Sr processed in the samples (typically  $\geq 200$  ng), so that no blank corrections were performed.

## 4. Results

### 4.1. Bioavailable Sr isotope composition and concentration range of Central Greece

The Sr concentrations and  $^{87}\text{Sr}/^{86}\text{Sr}$  values of the waters, plants and soil leachates are given in Table 1. The  $^{87}\text{Sr}/^{86}\text{Sr}$  values span a comparatively narrow range from 0.70768 to 0.71021, with the minimum and

maximum value observed for two soil leachates, respectively. The soil leachates define an average bioavailable  $^{87}\text{Sr}/^{86}\text{Sr}$  composition of  $0.70855 \pm 0.00060$  ( $n = 25, 1\sigma$ ), with bioavailable Sr concentrations (relative to dry unleached bulk soil) between 3.5 mg/kg and 34 mg/kg. The plant samples record a similar range in bioavailable  $^{87}\text{Sr}/^{86}\text{Sr}$  values between 0.70770 and 0.71016 with an average  $^{87}\text{Sr}/^{86}\text{Sr}$  value of  $0.70861 \pm 0.00055$  ( $n = 25, 1\sigma$ ). The plant Sr concentrations recorded values up to 110 mg/kg, but range typically from 2.5 mg/kg to 26 mg/kg.

The analysed surface and spring water  $^{87}\text{Sr}/^{86}\text{Sr}$  values range from 0.70769 to 0.70995 with average values of  $0.70831 \pm 0.00053$  ( $n = 15, 1\sigma$ ) and  $0.70835 \pm 0.00031$  ( $n = 17, 1\sigma$ ), respectively. The surface water Sr concentrations vary between 0.06 mg/l and 0.56 mg/l and the spring water Sr concentrations between 0.05 mg/l and 0.64 mg/l.

The  $^{87}\text{Sr}/^{86}\text{Sr}$  data reported here encompasses and slightly extends the range in previously published  $^{87}\text{Sr}/^{86}\text{Sr}$  values (0.70798–0.70916) for the study area (Hoogewerff et al., 2019; Voerkelius et al., 2010).

### 4.2. Distribution patterns and proxy variation

In order to study the inter- and intra-site specific proxy variation and to see whether the regional distribution in bioavailable  $^{87}\text{Sr}/^{86}\text{Sr}$  reflects the surface lithology of our study area, we plotted the Sr isotope compositions of the different environmental proxies sorted by sample site and surface lithology (Fig. 3). The grouping of the different sample sites based on their surface lithology reveals similar  $^{87}\text{Sr}/^{86}\text{Sr}$  ranges for both Cenozoic and Mesozoic sediments with average bioavailable  $^{87}\text{Sr}/^{86}\text{Sr}$  values of  $0.70844 \pm 0.00051$  ( $n = 39, 1\sigma$ ) and  $0.70852 \pm 0.00052$  ( $n = 43, 1\sigma$ ), respectively. Using Tukey's outlier test, which defines outliers as values that exceed more than 1.5 times the interquartile range from the quartiles (Tukey, 1977), the surface water, plant and soil leachate  $^{87}\text{Sr}/^{86}\text{Sr}$  values of site CG22 are identified as statistical outliers, suggesting that our data might overestimate the bioavailable  $^{87}\text{Sr}/^{86}\text{Sr}$  range typical for Mesozoic sediments to some extent.

Samples from areas dominated by Mesozoic and Cenozoic sediments are both characterised by fairly homogeneous  $^{87}\text{Sr}/^{86}\text{Sr}$  values with a maximum variation between  $^{87}\text{Sr}/^{86}\text{Sr}$  values of 0.0024 (Fig. 3). This is in agreement with previously published multi-proxy  $^{87}\text{Sr}/^{86}\text{Sr}$  data from the Peloponnese and Cyprus. In both locations inter-site proxy variation consistently  $<0.002$  between plants, soil leachates and waters were reported for areas characterised by sedimentary units (Frank et al., 2021; Ladegaard-Pedersen et al., 2019). In the current study, the surface and spring water  $^{87}\text{Sr}/^{86}\text{Sr}$  values vary generally by less than  $<0.0014$ , while the plants and soil leachates are characterised by maximum offsets of  $\sim 0.002$ . The different proxies from one site generally yielded  $^{87}\text{Sr}/^{86}\text{Sr}$  values within 0.0015 of each other for both the data from sites within Mesozoic and Cenozoic sediment dominated areas. The lowest intra-proxy variations are observed between the plants and soil leachates ( $\leq 0.0005$ ), while the largest (0.002) is found between the soil leachate and spring water samples of site CG22, which is located near the village of Kyrtoni (Fig. 1).

### 4.3. Cultural layers of Kirrha and Ayios Vasileios

The Sr concentrations and  $^{87}\text{Sr}/^{86}\text{Sr}$  values of the leached archaeological soils from the cultural layers of Kirrha and Ayios Vasileios are listed in Table 2. The cultural layers of Kirrha returned a very narrow range in  $^{87}\text{Sr}/^{86}\text{Sr}$  values from 0.70848 to 0.70856 with an average value of  $0.70854 \pm 0.00004$  ( $n = 7, 1\sigma$ ). The leached Sr concentrations (relative to dry unleached bulk soil) define a narrow range in bioavailable mobile Sr between 13.5 mg/kg and 16.6 mg/kg.

The cultural layers from Ayios Vasileios returned slightly higher and more variable bioavailable  $^{87}\text{Sr}/^{86}\text{Sr}$  values (0.70864–0.70901) with an average value of  $0.70883 \pm 0.00015$  ( $n = 4, 1\sigma$ ) and leached Sr concentrations (relative to dry unleached bulk soil) between 2.3 mg/kg and 4.3 mg/kg.

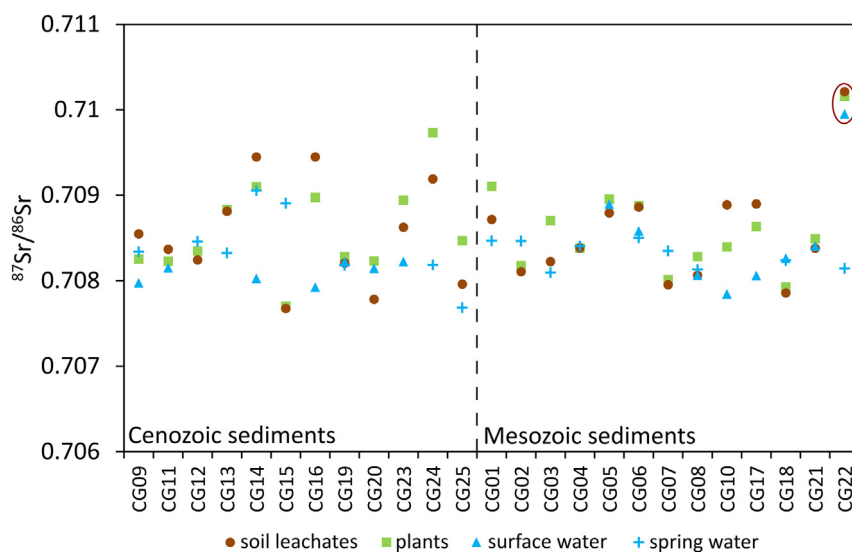


**Fig. 3.**  $^{87}\text{Sr}/^{86}\text{Sr}$  values measured for surface waters, spring waters, plants and soil leachates of the different sites sampled in Central Greece grouped based on the surface lithology present at the site. Outliers within the groupings were determined using Tukey's outlier test and are marked with red circles.

## 5. Discussion

### 5.1. Sources of bioavailable Sr on Central Greece

Bioavailable Sr can be sourced from endogenous sources, such as rocks and soils reflecting local geological background, as well as exogenous inputs, like atmospheric deposition and anthropogenic activities (e.g. Bentley, 2006; Capo et al., 1998; Frei and Frei, 2013). The bioavailable Sr fraction of Central Greece is likely a result of mixed Sr from several sources. To safely include the water, plant and soil leachate  $^{87}\text{Sr}/^{86}\text{Sr}$  signatures as baseline values for mobility studies, it is important to understand the processes and sources controlling their bioavailable Sr composition. Similarly, when investigating human mobility in archaeological studies, it is also essential to understand which bioavailable Sr sources are the ones that are most relevant to the human diet. Here, the concentrations of the different Sr sources play a significant role (e.g. Frei et al., 2020).

To determine the potential endmembers controlling the bioavailable  $^{87}\text{Sr}/^{86}\text{Sr}$  composition of Central Greece we created mixing diagrams plotting the  $^{87}\text{Sr}/^{86}\text{Sr}$  values of our investigated proxies against their respective Sr concentrations (Fig. 4). These diagrams reveal that the environmental proxies sampled from areas characterised by Cenozoic and Mesozoic sediments span a similar array, suggesting similar, or even overlapping, Sr sources for bedrock associations. Further, Fig. 4 shows no clear correlation between the Sr concentrations and  $^{87}\text{Sr}/^{86}\text{Sr}$  values of either proxy, which suggests that the bioavailable Sr signatures of Central Greece are determined by multiple (at least three) Sr sources. The Sr data of the different proxies appear to converge to a Sr-rich (low  $1/[\text{Sr}]$ ), unradiogenic Sr end-member. This Sr source is likely inherent in the local bedrock, which is dominated by typically unradiogenic, Sr-rich Mesozoic carbonates and Cenozoic sediments with clastic carbonate components (BGR, 2020; EGD, 2019). This is in good agreement with previously published studies that identified carbonates (e.g. limestones and dolomites) as a dominant endogenous source of bioavailable Sr in various parts of the world (Frei and Frei, 2011; Frei et al., 2020; Liu et al., 2013, 2016; Ryan et al., 2018; Zhang et al., 2019), and also in Greece (Frank et al., 2021; Nafplioti, 2011).

In some parts of Central Greece, rare outcrops of Mesozoic igneous rocks occur (BGR, 2020; EGD, 2019). These potentially constitute another endogenous source of Sr for these areas. Contribution of Sr from igneous (granitoid) rocks to the respective bioavailable fractions could hypothetically explain the anomalously high  $^{87}\text{Sr}/^{86}\text{Sr}$  values measured

for the soil leachate, plant and surface water sample of site CG22. However, the rocks present in areas that we categorize as 'igneous rocks' in Central Greece are mostly pertaining to ophiolitic sequences, which are expected to be characterised by unradiogenic bioavailable  $^{87}\text{Sr}/^{86}\text{Sr}$  signatures of  $\sim 0.704$ , values typical for oceanic basalts (Capo et al., 1998; Tommasini et al., 2018), rendering them an unlikely source for the anomalously high  $^{87}\text{Sr}/^{86}\text{Sr}$  values of CG22. Further, analyses from sample site CG18, which is characterised by similar bedrocks as site CG22, diverge in Sr isotope compositions from the latter site. The proxies from this site returned  $^{87}\text{Sr}/^{86}\text{Sr}$  values that are similar to those of Mesozoic carbonates, suggesting that the surrounding surface sediments contribute most of the bioavailable Sr to CG18, likely through localised atmospheric and riverine transport. This was also suggested by Frank et al. (2021), who found no significant Sr contributions from igneous rocks to the surface environment of the Peloponnese, but instead recorded  $^{87}\text{Sr}/^{86}\text{Sr}$  values typical for the nearest surface outcrop at sites characterised by igneous outcrops. Depending on the composition and mass of such local additions they would result in distinctly different Sr signatures, which could explain the different  $^{87}\text{Sr}/^{86}\text{Sr}$  values measured at CG18 and CG22. However, they are unlikely to significantly alter the Sr isotope compositions of areas dominated by Sr-rich surface outcrops, such as the carbonates and carbonate-derived clastic sediments found on Central Greece.

While the observed scatter in  $^{87}\text{Sr}/^{86}\text{Sr}$  values in Fig. 4 is likely mainly due to variable contributions from Mesozoic and Cenozoic sediments, the large scatter in Sr concentrations suggests the presence of one or more additional endmembers of low Sr concentration. In some areas, seawater-derived Sr has been identified as an important source of bioavailable Sr to the surface environment of areas exposed to the sea (Evans et al., 2010; Frei and Frei, 2013; Ryan et al., 2018; Whipkey et al., 2000). Marine salts are characterised by the Sr isotope composition that modern seawater has today ( $^{87}\text{Sr}/^{86}\text{Sr} = 0.7092$ ; Burke et al., 1982; McArthur et al., 2001) and these can be added to the surface environment directly through sea-spray and/or rain (Bentley, 2006; Evans et al., 2010; Montgomery, 2010). A rainwater sample taken on the Peloponnese recorded a  $^{87}\text{Sr}/^{86}\text{Sr}$  value of 0.70892 (Frank et al., 2021). While this one value likely underestimates the regional and seasonal variance expected for rainwater, it was chosen as the best possible representative for our study area due to a lack of other data. The rainwater in this area has a  $^{87}\text{Sr}/^{86}\text{Sr}$  value very similar to that of modern seawater suggesting that marine salts likely dominate the Sr composition of rainwater, with other aerosols, such as dust or biogenic material, playing a



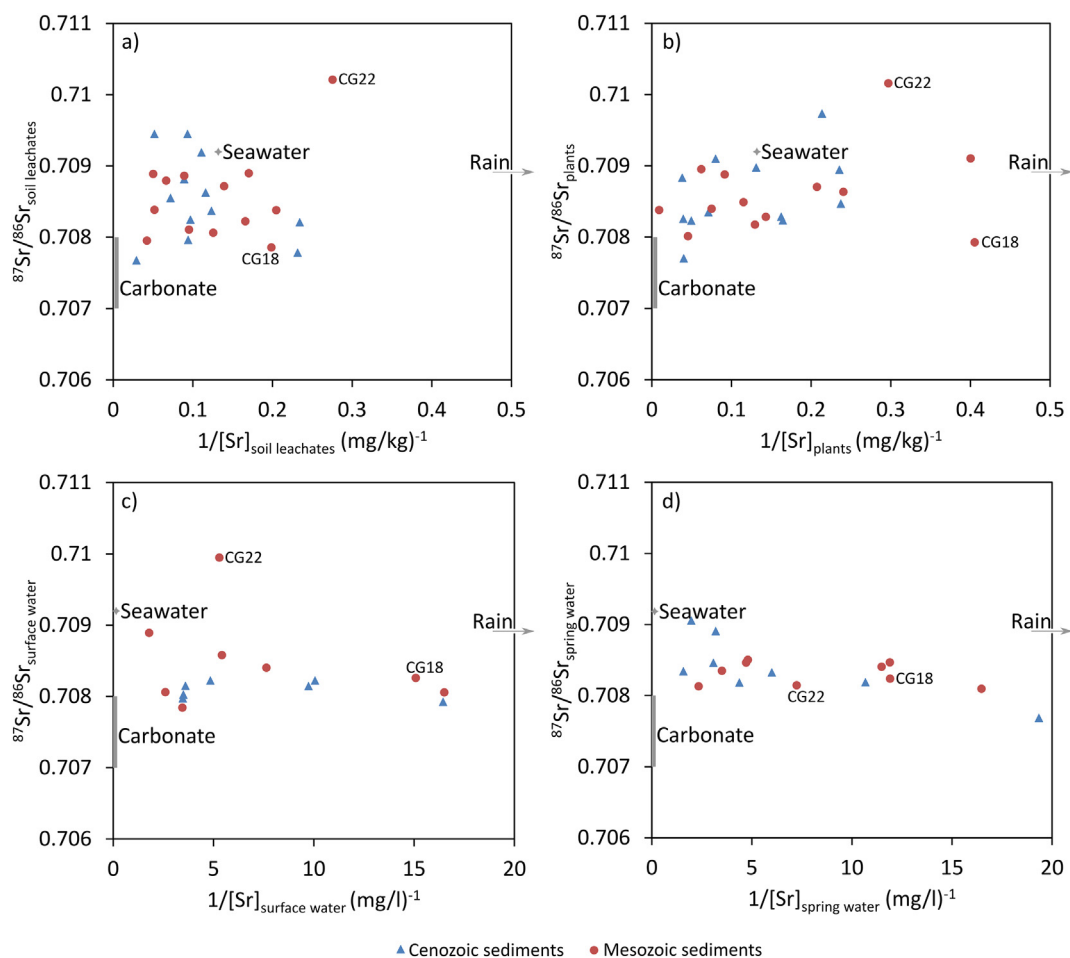


**Fig. 4.**  $^{87}\text{Sr}/^{86}\text{Sr}$  values of the soil leachate (a), plant (b), surface water (c) and spring water (d) samples plotted against their respective inverse Sr concentrations ( $1/[\text{Sr}]$ ). The Sr concentration and  $^{87}\text{Sr}/^{86}\text{Sr}$  values for carbonate, seawater and rain were based on data provided by Frank et al. (2021), McArthur et al. (2001) and Tommasini et al. (2018).

minor role. The addition of Sr via sea-spray and rainfall to the endogenous carbonate-sourced Sr likely accounts for the large scatter in Sr concentration observed in Fig. 4 as seawater and rain are characterised by comparatively low Sr concentrations (0.0001  $\mu\text{g}/\text{l}$ –383  $\mu\text{g}/\text{l}$ ; Capo et al., 1998; Tommasini et al., 2018). Its effect, if there is one, would be a pure dilution of the endogenous bioavailable Sr with little or no effect on its isotope compositions.

Besides the wet deposition of rain and sea-spray, the dry deposition of local and foreign dust may contribute to the composition of the Greek surface environment (Vasilatou et al., 2017). Foreign dust can originate from as far away as the Sahara Desert (e.g. Goudie and Middleton, 2001). Dust from this part of the world is yet another potential exogenous source of Sr, and is characterised by variable  $^{87}\text{Sr}/^{86}\text{Sr}$  signatures of 0.712 to 0.740 (Erel and Torrent, 2010; Grousset et al., 1998; Grousset and Biscaye, 2005). The Sr contribution from Saharan dust to the surface environment of Central Greece is likely highly variable and dependant on factors such as wind direction and relief. However, considering that the investigated proxies generally returned unradiogenic bioavailable  $^{87}\text{Sr}/^{86}\text{Sr}$  values ( $\leq 0.71$ ), the potential contribution of Sr derived from Saharan dust appears to play a minor role in determining the bioavailable  $^{87}\text{Sr}/^{86}\text{Sr}$  composition of Central Greece.

Finally, when trying to reconstruct past human mobility using a  $^{87}\text{Sr}/^{86}\text{Sr}$  baseline based on modern environmental samples, it is important to account for potential anthropogenic Sr contamination from agriculture and industry. Fertilisers, for example, have been shown to influence the  $^{87}\text{Sr}/^{86}\text{Sr}$  composition of waters and soils in some cases (Bentley, 2006; and references therein) and different types of fertilisers can introduce a wide range of Sr isotope signatures (0.705–0.711;

Hosono et al., 2007; Zieliński et al., 2016). The amounts and types of fertiliser used in Central Greece are not documented making it difficult to account for their potential contribution. Hence, we designed our sampling campaign to concentrate on sample locations on unfarmed, pristine land to limit fertiliser contamination. These sites appeared to be unaltered by human activity, however, a previous anthropogenic use and potential contamination cannot be completely excluded. Further, to achieve good geographical coverage, seven sites were sampled within agricultural areas (Supplement S2). Five of these are located within 10 km of pristine, non-agricultural sites, enabling us to better assess the difference in Sr isotope signatures and Sr concentrations between natural and agricultural sites. (Table 3). The surface and spring water samples generally returned higher Sr concentrations for the agricultural sites, which might be due to the addition of anthropogenic Sr. However, the same trend could not be observed for the soil samples. Further, the offset in water  $^{87}\text{Sr}/^{86}\text{Sr}$  values between natural and agricultural sites is generally  $\leq 0.00013$ , suggesting that any anthropogenic Sr added at the sampled agricultural sites did not significantly alter the pristine bioavailable  $^{87}\text{Sr}/^{86}\text{Sr}$  composition. The plants and soil leachates record  $^{87}\text{Sr}/^{86}\text{Sr}$  offsets of up to  $\sim 0.001$  between natural and agricultural sites, with the largest offset recorded for the plant samples of site CG01 and CG02. The pristine location, CG01, is located right beside the coast and returned a plant  $^{87}\text{Sr}/^{86}\text{Sr}$  value similar to modern seawater. This suggests that the offset between the plant and soil leachate values of CG01 and CG02 are more likely due to the addition of seawater-derived Sr to CG01 than to fertiliser use at CG02. The soil and plant leachate  $^{87}\text{Sr}/^{86}\text{Sr}$  values of the remaining pristine-agricultural site pairs are characterised by offsets  $\leq 0.0006$ . While this

**Table 3**

Comparison of  $^{87}\text{Sr}/^{86}\text{Sr}$  values and Sr concentrations measured for the plant, soil, surface water and spring water samples of agricultural and natural sites located within 10 km of each other.

Site pair	Distance (m)	Natural sites			Agricultural sites		
		Location	$^{87}\text{Sr}/^{86}\text{Sr}$	Sr (mg/kg)	Location	$^{87}\text{Sr}/^{86}\text{Sr}$	Sr (mg/kg)
<b>Plants</b>							
CG01-CG02	8.6	CG01	0.709106	2.50	CG02	0.708176	7.73
CG12-CG13	7.1	CG13	0.708833	26.23	CG12	0.708349	14.08
CG16-CG17	5.6	CG17	0.708636	4.16	CG16	0.708975	7.64
CG18-CG19	8.3	CG18	0.707927	2.47	CG19	0.708284	6.16
<b>Soil leachates</b>							
CG01-CG02	8.6	CG01	0.708718	7.19	CG02	0.708107	10.52
CG12-CG13	7.1	CG13	0.708814	11.23	CG12	0.708245	10.32
CG16-CG17	5.6	CG17	0.708900	5.88	CG16	0.709449	10.72
CG18-CG19	8.3	CG18	0.707857	5.04	CG19	0.708208	4.27
<b>Surface water</b>							
CG16-CG17	5.6	CG17	0.708057	0.06	CG16	0.707923	0.06
CG18-CG19	8.3	CG18	0.708261	0.07	CG19	0.708221	0.21
<b>Spring water</b>							
CG01-CG02	9.3	CG01	0.708468	0.08	CG02	0.708465	0.21
CG12-CG13	1.2	CG13	0.708325	0.17	CG12	0.708460	0.33
CG18-CG19	8.3	CG18	0.708239	0.08	CG19	0.708181	0.23

might be partially due to anthropogenic contamination, it could also be due to differences in the sites natural setting. This is supported by the comparatively large offsets in the plant and soil  $^{87}\text{Sr}/^{86}\text{Sr}$  signatures of two pristine sites (CG17 and CG18) only 4 km apart, which demonstrate that natural variations in  $^{87}\text{Sr}/^{86}\text{Sr}$  of up to 0.001 can occur in the study area over short distances. Differences in a sites setting that could contribute to these variations include, but are not limited to, local soil compositional differences, such as varying amounts of soil carbonates, differences in species-specific nutrient requirements as well as inhomogeneous contribution from exogenous Sr sources.

### 5.2. Differences in proxy $^{87}\text{Sr}/^{86}\text{Sr}$ signatures

Modern environmental samples have been increasingly used to determine bioavailable Sr isotope baselines for archaeological mobility studies (e.g. Evans et al., 2010; Evans and Tatham, 2004; Frei and Frei, 2011, 2013; Ladegaard-Pedersen et al., 2019, 2021; Montgomery, 2010). Different environmental proxies characterise the Sr isotope composition of different parts of the surface environment. Surface and spring water samples reflect the average bioavailable  $^{87}\text{Sr}/^{86}\text{Sr}$  signature of their catchment area, which can vary greatly depending on the geological background, hydrological properties and size of the catchment. Also, spring waters are likely dependent on the lithologies that predominate in their aquifers, as recently shown by a study of well drinking waters in Denmark (Frei et al., 2020). Plant and soil samples on the other hand are point samples, which represent the bioavailable  $^{87}\text{Sr}/^{86}\text{Sr}$  values at the immediate sample location. Further, water follows conservative mixing rules, while the Sr cycle within the soil-root system is rendered more complex by biological processes. Hence, the question about which environmental proxy is most suitable to create a reference baseline for bioavailable Sr for ancient mobility studies has been increasingly debated (Evans and Tatham, 2004; Frank et al., 2021; Frei and Frei, 2011, 2013; Ladegaard-Pedersen et al., 2019, 2021; Maurer et al., 2012; Ryan et al., 2018). Fig. 5 shows the pairwise correlation of our investigated proxies (surface water, spring water, plants and soil leachates) to better understand and assess the differences in their respective  $^{87}\text{Sr}/^{86}\text{Sr}$  values.

#### 5.2.1. Plants vs soil leachates

Most of the investigated plant and soil leachate  $^{87}\text{Sr}/^{86}\text{Sr}$  values fall along the 1:1 line of Fig. 5a revealing a strong positive correlation ( $R^2 = 0.768$ ). No clear divisive trend between the samples from

Cenozoic and Mesozoic sediment-dominated areas can be observed. Both sets of samples are characterised by a largely overlapping range in  $^{87}\text{Sr}/^{86}\text{Sr}$  values, by similar offsets in either direction compared to the 1:1 line, as well as by high positive inter-correlations ( $R^2 \geq 0.69$ ). The close relationship between plant and soil leachate  $^{87}\text{Sr}/^{86}\text{Sr}$  values is likely due to an isotopically homogeneous soil profile, considering that a wide variety of plant species with different rooting depth were sampled. This is supported by previous studies, which reported a similarly close relationship between soil leachates and different plant species in specific areas (Frank et al., 2021; Ladegaard-Pedersen et al., 2019; Nakano et al., 2001).

#### 5.2.2. Plants/soil leachates vs surface water

The plant vs surface water plot (Fig. 5b) looks similar to the soil leachate vs surface water plot (Fig. 5d). However, while the plant  $^{87}\text{Sr}/^{86}\text{Sr}$  values show a good correlation towards the surface water  $^{87}\text{Sr}/^{86}\text{Sr}$  values ( $R^2 = 0.542$ ), the soil leachates  $^{87}\text{Sr}/^{86}\text{Sr}$  values are only weakly correlated ( $R^2 = 0.253$ ). The plant and soil leachate  $^{87}\text{Sr}/^{86}\text{Sr}$  values are generally equal or greater compared to their respective surface water  $^{87}\text{Sr}/^{86}\text{Sr}$  values. This is particularly the case for the plant samples, where all but one location (CG09) recorded a plant  $^{87}\text{Sr}/^{86}\text{Sr}$  value lower than the respective surface water  $^{87}\text{Sr}/^{86}\text{Sr}$  value. The generally lower surface water  $^{87}\text{Sr}/^{86}\text{Sr}$  values, compared to the plants and soil leachates suggest a higher influence of unradiogenic carbonate Sr on the surface waters than on the plants and soils. This can be explained by the fact that the plant and soil leachates are point samples, whereas the surface waters reflect the average Sr compositions of larger catchment areas. Considering the high abundance of Sr-rich carbonates in Central Greece, the sampled surface waters likely picked up carbonate-sourced Sr within their catchment areas and transported this averaged out Sr isotope signature to the respective sampling sites, resulting in the observed offsets between surface water and plant/soil leachate  $^{87}\text{Sr}/^{86}\text{Sr}$  values at the investigated sites.

When comparing the surface water  $^{87}\text{Sr}/^{86}\text{Sr}$  values of samples from within areas dominated by Cenozoic- and Mesozoic sediments, they appear to be characterised by different trends compared to the plant and soil/leachate values (Fig. 5b+d). While the surface water  $^{87}\text{Sr}/^{86}\text{Sr}$  values from areas characterised by Mesozoic sediments tend to increase with increasing plant  $^{87}\text{Sr}/^{86}\text{Sr}$  signatures ( $R^2 = 0.819$ ) and soil leachate  $^{87}\text{Sr}/^{86}\text{Sr}$  values ( $R^2 = 0.568$ ), the surface water  $^{87}\text{Sr}/^{86}\text{Sr}$  values from areas with Cenozoic sediments define a cluster around a  $^{87}\text{Sr}/^{86}\text{Sr}$  value of  $\sim 0.708$  with no apparent correlation to respective plant/soil

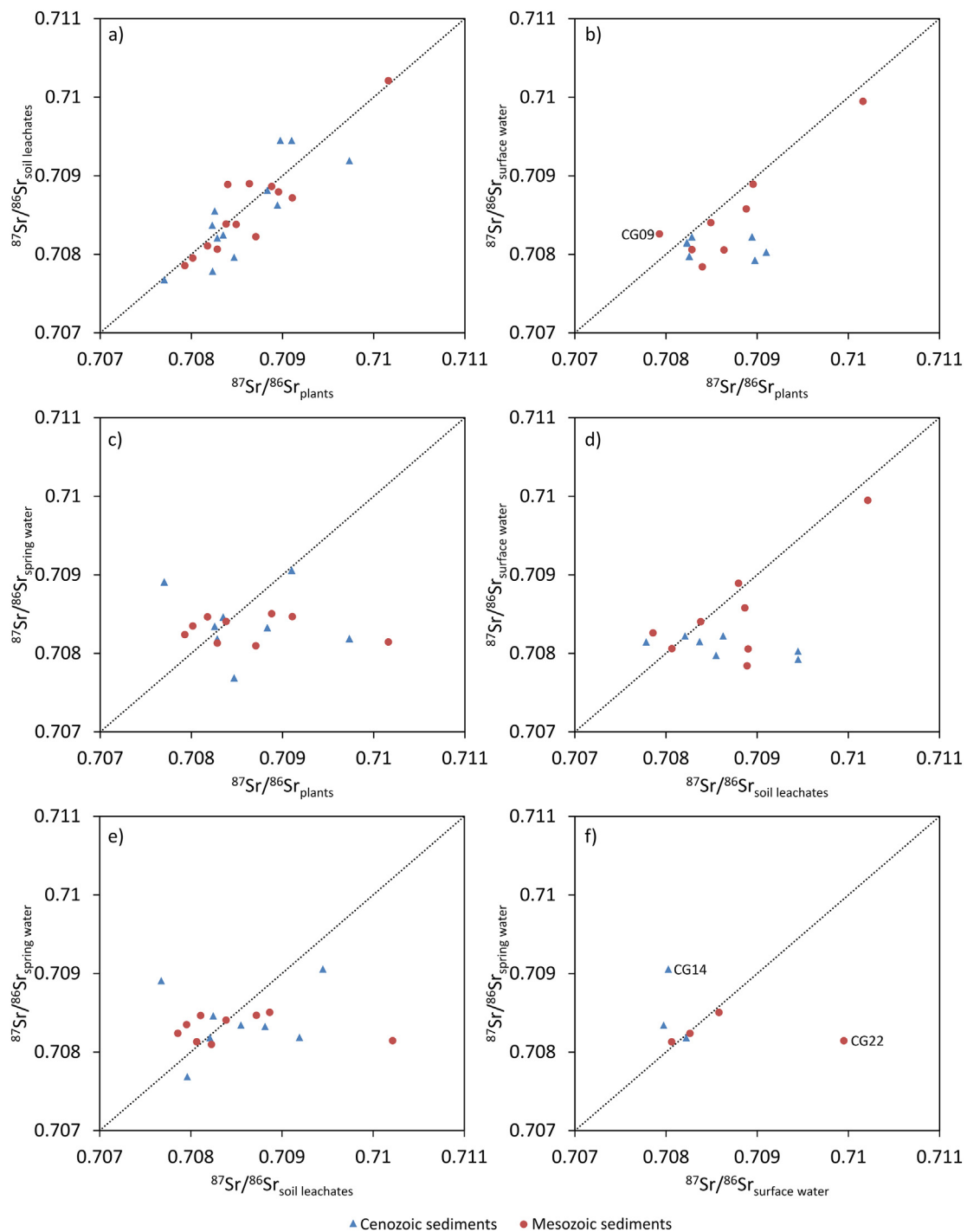


**Fig. 5.** Pairwise correlations between  $^{87}\text{Sr}/^{86}\text{Sr}$  ratios of plants and soil leachates (a), plants and surface water (b), plants and spring water (c), soil leachates and surface water (d), soil leachates and spring water (e) and surface water and spring water (f) at individual sites. The dotted lines mark the 1:1 line of perfect correlation.

leachate values. A  $^{87}\text{Sr}/^{86}\text{Sr}$  signature of  $\sim 0.708$  is very similar to seawater values present during the Cenozoic, which was likely incorporated in limestones and other carbonate sediments deposited during this period (McArthur et al., 2001). Hence, the surface waters from areas dominated by Cenozoic sediments likely receive a more pronounced Sr isotope signal from the weathering of these respective carbonates, which is then transported by creeks and rivers to the sampling sites.

### 5.2.3. Surface waters vs spring waters

Due to the arid conditions in Central Greece, surface waters could not be sampled at all sites. As a recent study on the Peloponnese

suggested that spring waters might serve as a substitute to surface waters in dry regions (Frank et al., 2021), we supplemented our water sample set with spring waters located within close proximity to sites without surface water. Further, additional spring water samples were taken close to seven sites with surface water in order to better assess the suitability of spring waters as a surface water substitute. While five of these sites fall on or close to the 1:1 line in the surface water vs spring water plot, two sites (CG14 & CG22) yield values which are significantly offset from each other (Fig. 5f). These explain the resulting poor correlation ( $R^2 = 0.101$ ) between surface and spring waters. The observed difference between the spring water  $^{87}\text{Sr}/^{86}\text{Sr}$  value and

surface water  $^{87}\text{Sr}/^{86}\text{Sr}$  value for site CG22 could be purely geographic as the spring water location is located ~6 km away from the surface water site. However, in case of site CG14, where a discrepancy between surface and spring water  $^{87}\text{Sr}/^{86}\text{Sr}$  signature also exists, the respective spring water sample was taken less than 1 km away from the surface water collection site. This suggests that significant differences in surface and spring water  $^{87}\text{Sr}/^{86}\text{Sr}$  signatures can occur over relatively short distances, which are likely caused by geological and hydrological differences between local aquifers and catchment areas.

#### 5.2.4. Plants/soil leachates vs spring waters

Fig. 5c+e reveals that the plant/soil leachate  $^{87}\text{Sr}/^{86}\text{Sr}$  values do not correlate with the spring water  $^{87}\text{Sr}/^{86}\text{Sr}$  values ( $R^2 \leq 0.015$ ). While the plants/soil leachate samples are characterised by a range in  $^{87}\text{Sr}/^{86}\text{Sr}$  values of 0.70768 to 0.71021, most of the spring water samples cluster around a  $^{87}\text{Sr}/^{86}\text{Sr}$  value of ~0.7083. The rather homogeneous spring water  $^{87}\text{Sr}/^{86}\text{Sr}$  signatures are likely the result of Sr from carbonate dominated aquifers as discussed above for the surface water samples from areas characterised by Cenozoic sediments. This is further supported by the relatively elevated Sr concentrations that are  $\geq 0.2$  mg/l for many of the spring and surface waters. It appears that local differences between sample sites, such as geological background and/or proximity to coastlines, are captured in the plant/soil leachate  $^{87}\text{Sr}/^{86}\text{Sr}$  signatures, but not so much in the spring waters, where we expect an averaging out of local  $^{87}\text{Sr}/^{86}\text{Sr}$  signatures to happen in the respective aquifers at depth. Unlike the surface waters, this averaging effect is also seen for spring waters sampled from areas characterised by Mesozoic sediments.

#### 5.2.5. Proxy evaluation

The range in intra-site proxy variation and different degrees of correlation between our investigated proxies demonstrate the need for comprehensive multi-proxy investigation to properly assess the bioavailable Sr isotope composition of an area (Figs. 3+5, Table 1). When trying to construct a suitable reference baseline for human mobility studies, it is paramount to understand the impact of potential local food and dietary sources. Humans derive Sr mainly through drinking water and plant-based foods as the Sr concentrations of animal-based foods are comparatively low (Coelho et al., 2017; Rose et al., 2010). Hence, plants and water samples are the obvious choice for constructing Sr isotope baselines to trace human mobility. Soil leachates on the other hand have been suggested to be less suitable as they were found to be quite variable on the regional scale and quite inconsistent with plant data on the local scale (Maurer et al., 2012). However, considering the close relationship between plant  $^{87}\text{Sr}/^{86}\text{Sr}$  values and soil leachate  $^{87}\text{Sr}/^{86}\text{Sr}$  values observed in this and previous studies (Frank et al., 2021; Ladegaard-Pedersen et al., 2019), we nevertheless consider soil leachates as a suitable reference substitute for the Sr sourced from plant-based food.

The spring waters sampled in this study correlate poorly with the other investigated proxies including the surface waters. Hence, they are likely not a good substitute for surface waters in Central Greece as they commonly diverge from the  $^{87}\text{Sr}/^{86}\text{Sr}$  signature of the surface environment. On the other hand, a study from Denmark reported a good agreement in Sr isotope signatures between major surface water archives and well drinking waters (Frei et al., 2020), emphasising that the applicability of spring waters as a surface  $^{87}\text{Sr}/^{86}\text{Sr}$  proxy is dependent on the regional setting. While spring waters might not reflect bioavailable  $^{87}\text{Sr}/^{86}\text{Sr}$  values typical for the surface environment of Central Greece it is important to remember that in such an arid area surface water resources might have been a limited resource for human drinking water due to their scarcity. Hence, spring water  $^{87}\text{Sr}/^{86}\text{Sr}$  data might still be relevant for inclusion in baseline characterisation as waters from springs were likely preferably consumed by ancient humans living in deserted areas, as they do today.

### 5.3. Defining bioavailable $^{87}\text{Sr}/^{86}\text{Sr}$ baselines for Greece

In order to conduct meaningful investigations of ancient human mobility, it is imperative to define robust bioavailable Sr isotope baselines of suspected areas of origin. As discussed in Section 2.2, quite a bit of bioavailable Sr baseline data has been published for Greece over the last years (Bishop et al., 2020; Frank et al., 2021; Hoogewerff et al., 2019; Leslie, 2012; Nafplioti, 2008, 2011; Panagiotopoulou et al., 2018; Richards et al., 2008; Triantaphyllou et al., 2015; Vaiglova et al., 2018; Voerkelius et al., 2010; Wang et al., 2019; Whelton et al., 2018). However, no comprehensive bioavailable Sr baselines exist for Greece as a whole to this date. Further, most of the above cited studies focused strongly on the Sr isotope signatures of individuals, and are not dedicated to establishing robust baselines against which the human signatures can be compared to. In the following, we attempt to remedy this by combining our bioavailable Sr isotope data from Central Greece with the already published baseline data.

We provide Sr bioavailable baselines for the different administrative regions of Greece, suitable to enable respective regional provenance investigations. Further, we present bioavailable Sr baselines for the main surface lithologies found in Greece, as the modern administrative regions are likely not representative of ancient Greece and as bioavailable  $^{87}\text{Sr}/^{86}\text{Sr}$  signatures in Greece have been shown to heavily depend on the surface lithology (Frank et al., 2021; Nafplioti, 2011). The baselines were established using baseline data that are representative of bioavailable fractions only, excluding previously published bulk rock data. The proxies used include bones of archaeological humans, faunal remains, modern faunal samples as well as modern environmental samples (Supplement S4). The different proxy types all have the possibility to

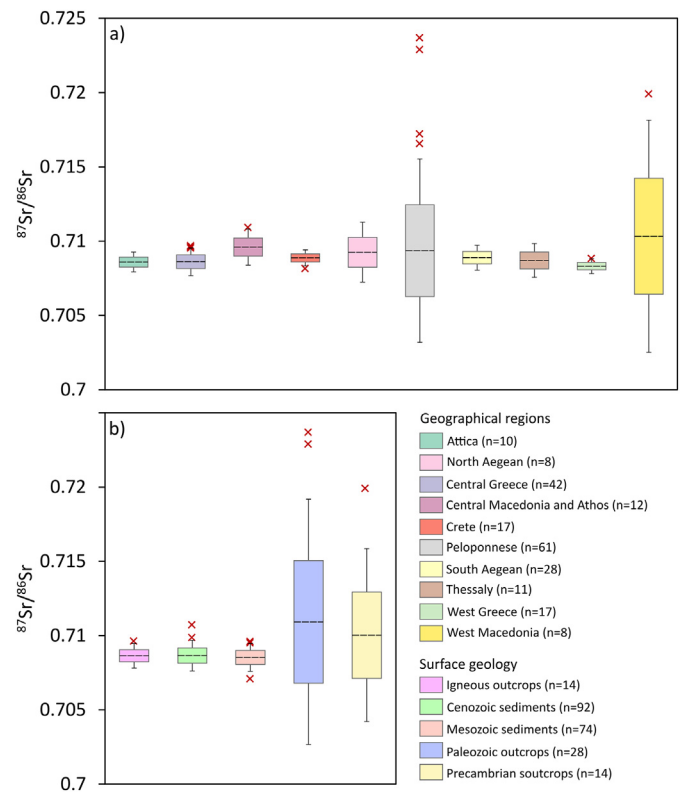


**Fig. 6.** Bioavailable Sr isotope baselines for the different geographical regions (a) and surface lithologies (b) of Greece calculated as the average  $^{87}\text{Sr}/^{86}\text{Sr}$  composition (dotted line) of their available bioavailable  $^{87}\text{Sr}/^{86}\text{Sr}$  data  $\pm$  their respective single ( $\sigma$ ; boxes) and double standard deviation ( $2\sigma$ ; whiskers). Reported  $^{87}\text{Sr}/^{86}\text{Sr}$  data that falls outside of their respective baseline range are given as red crosses.

be biased away from the  $^{87}\text{Sr}/^{86}\text{Sr}$  isotope signature of the human diet. The modern environmental samples could be influenced by modern day human activity, while both archaeological and modern human and faunal remains could potentially reflect migration in themselves. However, as in this study, the cited publications took caution to account for potential biases in their baseline  $^{87}\text{Sr}/^{86}\text{Sr}$  data, so that we consider the different proxy data reliable. In cases where one site is characterised by several  $^{87}\text{Sr}/^{86}\text{Sr}$  values from one or several proxies (e.g. Frank et al., 2021; Panagiotopoulou et al., 2018; Vaiglova et al., 2018), their average  $^{87}\text{Sr}/^{86}\text{Sr}$  value was calculated to characterise the respective site. This was done to ensure that every site was equally weighed when calculating our bioavailable Sr isotope baselines. Finally, as many studies did not include GPS coordinates for their sampling sites (e.g. Nafplioti, 2011; Panagiotopoulou et al., 2018; Whelton et al., 2018), their coordinates had to be approximated based on the information provided by the respective studies. This introduces some degree of uncertainty to the grouping of the samples based on their respective region and surface geology.

When establishing reference baselines for a region for the purpose of mobility studies it is common to define the baselines as the average bioavailable  $^{87}\text{Sr}/^{86}\text{Sr}$  signature of that region  $\pm$  its single ( $\bar{x} \pm \sigma$ ) or double standard deviation ( $\bar{x} \pm 2\sigma$ ). We calculated both, but will in the following focus on the baselines defined by their double standard deviations to ensure a broader, more conservative applicability of our baselines (Fig. 6). For regions and surface lithologies, which are characterised by less than five sampling sites, no baselines were calculated. Finally, it is important to note, that our baselines are meant as a first attempt to better characterise the bioavailable Sr isotope composition of the Greek surface environment to provide future mobility studies with a better understanding of the range in bioavailable  $^{87}\text{Sr}/^{86}\text{Sr}$  values. They should be regarded as a starting point for future sampling campaigns. Certainly, depending on the target area and goal of such studies, additional sampling is necessary to achieve a higher spatial resolution.

### 5.3.1. Geographical distribution of bioavailable $^{87}\text{Sr}/^{86}\text{Sr}$ signatures

Of the 13 administrative regions of Greece (Central Macedonia and Athos were considered as one, due to the small size of the latter), bioavailable Sr isotope baselines could be defined for ten of them (Fig. 6a). The resulting baselines show a wide range in bioavailable  $^{87}\text{Sr}/^{86}\text{Sr}$  values, with the narrowest baseline observed for West Greece and the highest variability observed for West Macedonia.

The bioavailable Sr isotope baseline of West Greece is tentatively calculated as  $0.70832 \pm 0.00049$  ( $\bar{x} \pm 2\sigma$ ;  $n = 17$ ) encompassing all published Sr data for West Greece but one soil sample (Hoogewerff et al., 2019). However, the offset between this soil leachate  $^{87}\text{Sr}/^{86}\text{Sr}$  value and the upper baseline range is  $<0.00003$ , rendering the baseline a decent fit for assessing the regional bioavailable  $^{87}\text{Sr}/^{86}\text{Sr}$  signature of West Greece.

Crete is characterised by a similarly narrow bioavailable Sr baseline range of  $0.70888 \pm 0.00054$  ( $\bar{x} \pm 2\sigma$ ;  $n = 17$ ). One spring water from Crete yielded a  $^{87}\text{Sr}/^{86}\text{Sr}$  value  $\sim 0.002$  lower than the lower baseline range (Voerkelius et al., 2010), suggesting that the calculated baseline underestimates the total range in  $^{87}\text{Sr}/^{86}\text{Sr}$  found on Crete. As also seen in this study, spring waters can record a distinctly different  $^{87}\text{Sr}/^{86}\text{Sr}$  signature than surface waters or other surface proxies as they might tap deeper aquifers that sit in lithologically different strata. Hence, additional sampling of spring water might be necessary for future mobility studies on Crete, if the archaeological context provides evidence of water usage from wells.

The  $^{87}\text{Sr}/^{86}\text{Sr}$  baseline of Central Greece completely encompasses the baseline ranges of West Greece and Crete with a range in bioavailable Sr of  $0.70862 \pm 0.00092$  ( $\bar{x} \pm 2\sigma$ ;  $n = 42$ ). Despite the wider baseline range, four sites in Central Greece returned  $^{87}\text{Sr}/^{86}\text{Sr}$  values up to 0.00016 higher than the upper baseline range. Two of these sites were soils sampled from Palaeozoic outcrops on the island Euboea (Hoogewerff et al., 2019), which are expected to be characterised by

more radiogenic  $^{87}\text{Sr}/^{86}\text{Sr}$  values. Hence, the elevated  $^{87}\text{Sr}/^{86}\text{Sr}$  values of these sites are likely due to natural variation in the surface lithology. The other two sites are located both on Mesozoic sediments, suggesting that their elevated  $^{87}\text{Sr}/^{86}\text{Sr}$  value compared to the calculated baseline might not be caused by the surface lithology of the site (this study; Prevedorou, 2015). One of these sites is CG22 from this study. As the anomalously high bioavailable  $^{87}\text{Sr}/^{86}\text{Sr}$  values measured at this site are likely the result of natural variations in Sr input, the calculated baseline for Western Greece might slightly underestimate the total range in bioavailable  $^{87}\text{Sr}/^{86}\text{Sr}$  typical for Central Greece.

The region of Central Macedonia and Athos is characterised by a bioavailable  $^{87}\text{Sr}/^{86}\text{Sr}$  baseline of  $0.70960 \pm 0.00122$  ( $\bar{x} \pm 2\sigma$ ;  $n = 12$ ). For one agricultural soil in Central Macedonia, a positive offset of  $-0.0001$  compared to the upper baseline range was reported (Hoogewerff et al., 2019). This could be due to anthropogenic contamination in the agricultural soil, but is more likely the result of the highly variable surface lithology in Central Macedonia, as the soil is developed on Precambrian outcrops.

The  $^{87}\text{Sr}/^{86}\text{Sr}$  baselines of the Peloponnese and West Macedonia are calculated as  $0.70936 \pm 0.00617$  ( $\bar{x} \pm 2\sigma$ ;  $n = 62$ ) and  $0.71033 \pm 0.00780$  ( $\bar{x} \pm 2\sigma$ ;  $n = 8$ ), respectively. On the Peloponnese four sites and in West Macedonia one site returned  $^{87}\text{Sr}/^{86}\text{Sr}$  values significantly above their respective upper baseline range with offsets of up to  $\sim 0.008$  (Frank et al., 2021; Hoogewerff et al., 2019). These sites are all located within areas characterised by Palaeozoic or Precambrian outcrops, suggesting that these outlier-like values are due to natural variations within the surface lithology. Further, due to the high variability in  $^{87}\text{Sr}/^{86}\text{Sr}$  values observed in both regions, their calculated baselines are characterised by very wide ranges. These might seem unsuitable for investigating mobility within Greece as they encompass the  $^{87}\text{Sr}/^{86}\text{Sr}$  isotope signatures of all the other regions. Hence, when investigating mobility within the Peloponnese or West Macedonia it might be appropriate to redefine their respective baselines using only their single standard deviation or to define regionally smaller baselines within the Peloponnese or West Macedonia.

The  $^{87}\text{Sr}/^{86}\text{Sr}$  data from Attica and the South Aegean define rather narrow Sr bioavailable baseline ranges of  $0.70859 \pm 0.00066$  ( $\bar{x} \pm 2\sigma$ ;  $n = 10$ ) and  $0.70889 \pm 0.00083$  ( $\bar{x} \pm 2\sigma$ ;  $n = 28$ ), respectively. On the other hand, Thessaly and the North Aegean are characterised by slightly wider baseline ranges in bioavailable  $^{87}\text{Sr}/^{86}\text{Sr}$  values of  $0.70870 \pm 0.00113$  ( $\bar{x} \pm 2\sigma$ ;  $n = 11$ ) and  $0.70925 \pm 0.00201$  ( $\bar{x} \pm 2\sigma$ ;  $n = 8$ ), respectively. All four baselines encompass all of the  $^{87}\text{Sr}/^{86}\text{Sr}$  data published for their respective regions to date, suggesting that the baselines are a good approximation of the ranges in  $^{87}\text{Sr}/^{86}\text{Sr}$  values typical for Attica, the North and South Aegean and Thessaly.

Fig. 2 reveals that the baseline sampling sites cover the different administrative regions of Greece unevenly. While the South Aegean and the Peloponnese are thoroughly explored with sampling densities of 53 and 39 sites per  $10,000\text{km}^2$ , northern Greece is underrepresented with sampling densities consistently below 10 sites per  $10,000\text{km}^2$ . For the administrative regions East Macedonia and Thrace, Epirus and the Ionian Islands too few  $^{87}\text{Sr}/^{86}\text{Sr}$  data is available to date to calculate statistically sound baselines. The data points published for these regions only give a first estimate of what the bioavailable Sr composition in these regions could be like (Supplement S4). The calculated baselines for Central Macedonia and Athos, West Macedonia and Thessaly are based on sampling densities between 6 and 8.5 sites per  $10,000\text{km}^2$ . Considering the complex surface lithology of northern Greece (Fig. 1), such sampling site densities are likely insufficient to adequately capture the complete variability in Sr isotope compositions. Hence, additional sampling should be conducted in these regions in order to better characterise their bioavailable baseline  $^{87}\text{Sr}/^{86}\text{Sr}$  range. Future mobility studies without the means to conduct additional sampling in these areas could alternatively use the statistical, bioavailable  $^{87}\text{Sr}/^{86}\text{Sr}$  ranges based on the surface lithology of Greece, which will be discussed in the following.

### 5.3.2. Bioavailable $^{87}\text{Sr}/^{86}\text{Sr}$ signatures and the geological background

Environmental proxy data grouped into the five main surface lithology groups found in Greece returned distinctly different statistical Sr isotopic signatures (Fig. 6b). The areas characterised by Cenozoic and Mesozoic sediments are characterised by unradiogenic, narrowly defined bioavailable  $^{87}\text{Sr}/^{86}\text{Sr}$  ranges, which is in good agreement with previously reported Sr isotope baseline data from other Mediterranean regions (Cavazzuti et al., 2019; Frank et al., 2021; Ladegaard-Pedersen et al., 2019). Locations within igneous outcrops returned a bioavailable Sr isotope range similar to that of the Cenozoic and Mesozoic sediments with a rather unradiogenic average  $^{87}\text{Sr}/^{86}\text{Sr}$  value and a narrow baseline range. The bioavailable  $^{87}\text{Sr}/^{86}\text{Sr}$  signature ranges of the areas dominated by Palaeozoic and Precambrian rock outcrops on the other hand are defined by more radiogenic  $^{87}\text{Sr}/^{86}\text{Sr}$  averages and wide ranges in  $^{87}\text{Sr}/^{86}\text{Sr}$  values.

The sites located within Cenozoic sediment dominated areas define a bioavailable Sr isotope range of  $0.70866 \pm 0.00082$  ( $\bar{x} \pm 2\sigma$ ;  $n = 92$ ) for all of Greece. This statistical range covers all of the bioavailable Sr data reported for samples from Cenozoic sediments, except for one soil leachate  $^{87}\text{Sr}/^{86}\text{Sr}$  value from West Macedonia and one animal teeth  $^{87}\text{Sr}/^{86}\text{Sr}$  value from Central Macedonia (Hoogewerff et al., 2019; Whelton et al., 2018). These values are slightly more radiogenic than the calculated baseline range, suggesting that the latter underestimates the total range in  $^{87}\text{Sr}/^{86}\text{Sr}$  that can occur within areas characterised by Cenozoic sediments. However, both samples were taken within close proximity to Palaeozoic and/or Precambrian outcrops, which are commonly characterised by more radiogenic  $^{87}\text{Sr}/^{86}\text{Sr}$  values (e.g. Capo et al., 1998; Tommasini et al., 2018). Hence, the positive offset of up to 0.001 between the baseline compositional range and the values from West and Central Macedonia is likely a result of mixing of Sr sources along the outcrop boundary.

Just as in Central Greece, sites in areas dominated by Mesozoic sediments across entire Greece are defined by a very similar range in bioavailable  $^{87}\text{Sr}/^{86}\text{Sr}$  as those from areas dominated by Cenozoic sediments. The statistical range in  $^{87}\text{Sr}/^{86}\text{Sr}$  signatures of samples from areas characterised by Mesozoic sediments is calculated as  $0.70853 \pm 0.00094$  ( $\bar{x} \pm 2\sigma$ ;  $n = 74$ ), which covers most of the reported bioavailable  $^{87}\text{Sr}/^{86}\text{Sr}$  data from these areas. However, at four sites,  $^{87}\text{Sr}/^{86}\text{Sr}$  values outside of the calculated baseline range were reported (This study; Frank et al., 2021; Hoogewerff et al., 2019; Prevedorou, 2015). An agricultural soil sample from the Peloponnese returned a  $^{87}\text{Sr}/^{86}\text{Sr}$  value  $-0.002$  lower than the lower range of the baseline (Hoogewerff et al., 2019). In the same study a soil leachate  $^{87}\text{Sr}/^{86}\text{Sr}$  value for a grazing land soil, which is located less than 1 km away from the corresponding agricultural soil, is reported as being characterised by a  $^{87}\text{Sr}/^{86}\text{Sr}$  value of 0.70888. This falls within the herein defined Sr isotope range, suggesting that the low  $^{87}\text{Sr}/^{86}\text{Sr}$  value of the agricultural soil might be due to anthropogenic contamination. The other three sites that fall outside the calculated  $^{87}\text{Sr}/^{86}\text{Sr}$  range for areas with Mesozoic sediments returned positive upsets of up to 0.00023 for their environmental proxies. One of these sites is site CG22 from this study. As discussed above, the higher bioavailable  $^{87}\text{Sr}/^{86}\text{Sr}$  values of CG22 are likely caused by local differences in Sr input, which emphasises the need of spatially tight sampling campaigns when investigating local variabilities in bioavailable Sr.

The statistical range of bioavailable Sr isotope signatures for areas characterised by igneous outcrops in Greece is calculated as  $0.70865 \pm 0.00082$  ( $\bar{x} \pm 2\sigma$ ;  $n = 14$ ). This is surprisingly narrow as igneous rocks are expected to be characterised by a wide range in  $^{87}\text{Sr}/^{86}\text{Sr}$  values depending on their age and initial Rb/Sr value (e.g. Capo et al., 1998; Tommasini et al., 2018). Frank et al. (2021) as well as this study suggest that the contribution of bioavailable Sr to the surface environment from weathering of igneous rocks might be limited on the Peloponnese and Central Greece, where the bioavailable fractions seem to be more influenced by Sr released from neighbouring lithologies and/or are overprinted by exogenous Sr sources. This appears to apply for Greece as a whole as well, as most of the sites on igneous outcrops are located on the Aegean Islands, which generally yield bioavailable  $^{87}\text{Sr}/^{86}\text{Sr}$  values close to that of modern seawater (0.7092; Burke et al., 1982; McArthur et al., 2001).

Further, the one site in the South Aegean that yielded a  $^{87}\text{Sr}/^{86}\text{Sr}$  value slightly above the upper  $^{87}\text{Sr}/^{86}\text{Sr}$  range calculated for areas characterised by igneous outcrops, is located in close proximity to Palaeozoic outcrops, suggesting mixing between unradiogenic seawater sourced Sr and more radiogenic Sr sourced from these older rock outcrops.

The sites located within Palaeozoic outcrops returned a broad bioavailable Sr isotope signature range of  $0.71092 \pm 0.00826$  ( $\bar{x} \pm 2\sigma$ ;  $n = 28$ ). Frank et al. (2021) reported  $^{87}\text{Sr}/^{86}\text{Sr}$  values up to 0.0045 above the upper baseline range for two water samples from Palaeozoic outcrops on the Peloponnese, suggesting that the calculated baseline range underestimates the total range of  $^{87}\text{Sr}/^{86}\text{Sr}$  typical for these areas. The latter study generally found a trend towards more radiogenic water  $^{87}\text{Sr}/^{86}\text{Sr}$  values compared to soil leachate and plant  $^{87}\text{Sr}/^{86}\text{Sr}$  values when sampling within Palaeozoic outcrops, which emphasises the importance of multi-proxy sampling to capture the full range in bioavailable  $^{87}\text{Sr}/^{86}\text{Sr}$  signatures.

The sites dominated by Precambrian outcrops are also characterised by very heterogeneous bioavailable  $^{87}\text{Sr}/^{86}\text{Sr}$  signatures resulting in a broad statistical  $^{87}\text{Sr}/^{86}\text{Sr}$  range of  $0.71003 \pm 0.00582$  ( $\bar{x} \pm 2\sigma$ ;  $n = 14$ ). The lower average  $^{87}\text{Sr}/^{86}\text{Sr}$  value and statistical range observed for the Precambrian outcrops compared to the Palaeozoic outcrops is surprising as the first are expected to be more radiogenic due to their geological age. For example, a recent study constraining bioavailable  $^{87}\text{Sr}/^{86}\text{Sr}$  signatures for southern Sweden recorded  $^{87}\text{Sr}/^{86}\text{Sr}$  values up to 0.73823 for plants sampled from Precambrian outcrops (Ladegaard-Pedersen et al., 2021). One sample site in West Macedonia returned a soil leachate  $^{87}\text{Sr}/^{86}\text{Sr}$  value 0.00408 higher than the upper statistical  $^{87}\text{Sr}/^{86}\text{Sr}$  range calculated herein (Hoogewerff et al., 2019), further supporting that more radiogenic  $^{87}\text{Sr}/^{86}\text{Sr}$  values can be expected for areas characterised by Precambrian outcrops in Greece. Hence, additional sampling within these areas might be necessary to fully capture their typical range in  $^{87}\text{Sr}/^{86}\text{Sr}$ .

As for the baselines of the Peloponnese and West Macedonia, our applied method of defining the average bioavailable Sr isotope signatures for the different surface lithology groups as the average  $^{87}\text{Sr}/^{86}\text{Sr}$  value of all sites from each group  $\pm$  their double standard deviation ( $\bar{x} \pm 2\sigma$ ), resulted in very wide  $^{87}\text{Sr}/^{86}\text{Sr}$  ranges for areas characterised by Palaeozoic and Precambrian outcrops. These completely encompasses the  $^{87}\text{Sr}/^{86}\text{Sr}$  range of the igneous outcrops and Mesozoic and Cenozoic sediments. Hence, future studies on human mobility within or near Palaeozoic and Precambrian outcrops might want to redefine their respective baselines depending on the aims of the study. This could, for example, be done by using only specific proxies.

### 5.3.3. Evaluating the applicability of the defined baselines for ancient mobility studies

The Sr isotope composition of the cultural layers of two Bronze Age cemeteries, Kirrha and Ayios Vasileios, were compared to our calculated geographical and geological baselines (Fig. 7). This was done to test the applicability of our defined baselines for tracing mobility at actual archaeological sites. As the baselines aim to constrain the  $^{87}\text{Sr}/^{86}\text{Sr}$  fraction of the human diet a comparison to soil  $^{87}\text{Sr}/^{86}\text{Sr}$  values of Bronze Age farm land would be more ideal. However, the location of these are largely unknown rendering the cultural layers of the cemeteries the best possible approximation of bioavailable  $^{87}\text{Sr}/^{86}\text{Sr}$  values prevalent during the Bronze Age.

The cemetery of Kirrha is located on Mesozoic sediments in Central Greece (Fig. 1). The soil leachates from the different graves returned a narrow range in  $^{87}\text{Sr}/^{86}\text{Sr}$  signature between 0.70848 and 0.70859, which fall within the calculated baseline for the Mesozoic sediments of Greece and the regional baseline for Central Greece. Ayios Vasileios, which is located on Cenozoic Sediments on the Peloponnese returned a slightly wider range in  $^{87}\text{Sr}/^{86}\text{Sr}$  signature (0.70864–0.70901). This range is covered by the wide Sr isotope baseline calculated for the Peloponnese, but also by the significantly narrower baseline of the Cenozoic sediments. As discussed above, the wide baseline range of the

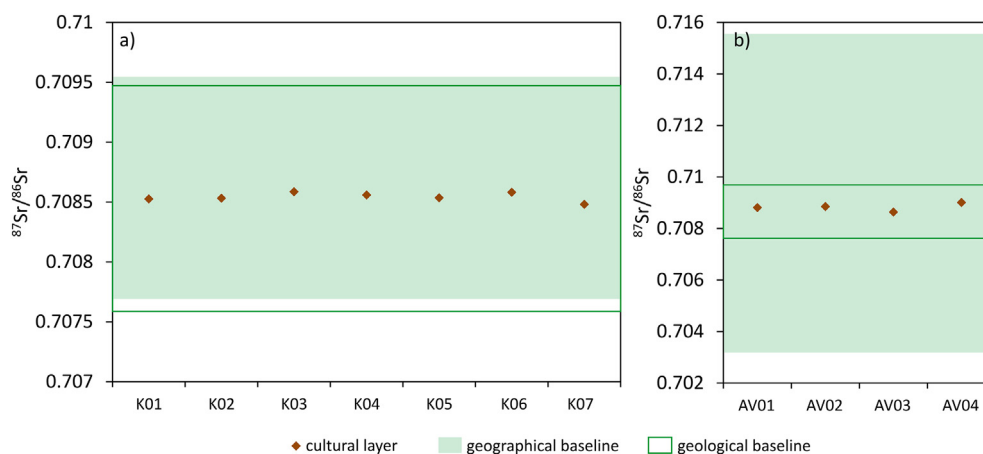


Fig. 7. Soil leachate  $^{87}\text{Sr}/^{86}\text{Sr}$  data from the cultural layers of Kirrha (a) and Ayios Vasileios (b) compared to their respective geographical and geological bioavailable Sr isotope baselines.

Peloponnese might seem unsuitable for mobility investigations and might need to be redefined based on the aims of future mobility studies. As in the above discussion, Fig. 7 compares the soil leachate  $^{87}\text{Sr}/^{86}\text{Sr}$  signature from Kirrha and Ayios Vasileios to the geographical and geological  $^{87}\text{Sr}/^{86}\text{Sr}$  signatures based on the double standard deviation ( $2\sigma$ ). However, the geographical and geological ranges defined by their average  $^{87}\text{Sr}/^{86}\text{Sr}$  value  $\pm$  their respective single standard deviation ( $\sigma$ ) also encompass the complete variation in  $^{87}\text{Sr}/^{86}\text{Sr}$  values measured for the cultural layers from Kirrha and Ayios Vasileios, supporting the applicability of our calculated baselines for identifying (non-)locals to Greece.

The geographical baselines in this study were defined to identify 1) inter-regional mobility within Greece as well as 2) locals to Greece. However, while the cultural layers of Kirrha and Ayios Vasileios returned distinctly different  $^{87}\text{Sr}/^{86}\text{Sr}$  values, their respective geographical baselines are characterised by significant overlap as both are dominated by carbonate-like  $^{87}\text{Sr}/^{86}\text{Sr}$  values (0.707–0.709, McArthur et al., 2001). The baselines defined for the other regions of Greece herein also show an overlap with carbonate-like values to varying degrees. This reveals that the identification of mobility between the different regions of Greece with the geographical baselines is limited to individuals characterised by a  $^{87}\text{Sr}/^{86}\text{Sr}$  signature either below or above the overlapping range. When trying to investigate at a smaller, intraregional scale, the geographical baselines are not suitable, but, within geologically complex regions, such as the Peloponnese or West Macedonia, the statistically defined geological  $^{87}\text{Sr}/^{86}\text{Sr}$  signature can be used to determine mobility. As the geographical baselines, their applicability is limited by an overlap at carbonate-like values though. Future mobility studies investigating mobility at the intraregional scale within Greece might be able to reduce the overlap by re-defining geologically based Sr isotope baselines for the region they are investigating as was done by Frank et al. (2021) for the Peloponnese.

The applicability of the statistically defined geographical and geological bioavailable  $^{87}\text{Sr}/^{86}\text{Sr}$  ranges to identify locals to Greece is also limited, as they overlap with  $^{87}\text{Sr}/^{86}\text{Sr}$  baselines reported for other Mediterranean areas, such as Cyprus and northern Italy (Cavazzuti et al., 2019; Ladegaard-Pedersen et al., 2019). Future mobility studies faced with this limitation should therefore consider additional data, such as other provenance proxies or the archaeological context, when investigating individual mobility in Greece.

## 6. Conclusion

In this study we present Sr isotope signatures and concentrations for plant, soil leachate and spring and surface water samples from Central Greece and combine them with previously published bioavailable  $^{87}\text{Sr}/^{86}\text{Sr}$  data from all of Greece in order to define the first extensive

bioavailable Sr isotope baseline for the different regions and surface lithologies of Greece. Our conclusions can be summarised as follows:

- 1) The Sr isotope compositions of the different investigated proxies from Central Greece are largely controlled by the weathering of surface lithologies, in particular of carbonates. The contribution of foreign Sr to the biosphere, such as from rain, sea-spray and dust, could not be assessed, however their potential contributions did not seem to have considerable effects on the Sr isotope compositions of the biosphere.
- 2) The surface and spring water samples generally returned quite narrowly ranged  $^{87}\text{Sr}/^{86}\text{Sr}$  ranges that are compatible with a significant contribution from carbonate-derived Sr. This is also reflected by their relatively elevated Sr concentrations typically around 0.2 mg/l. Small variations between Sr isotope signatures of surface and spring waters are likely due to differences in the characteristics of lithological sources present in their catchments and aquifers, and their respective role in influencing the average Sr isotope signature of the sampled waters. The plants and soil leachates are characterised by a slightly wider range in  $^{87}\text{Sr}/^{86}\text{Sr}$  values but generally reflect the compositional tenor of the surface and spring waters.
- 3) We present statistical, bioavailable  $^{87}\text{Sr}/^{86}\text{Sr}$  ranges for the different administrative regions and surface lithologies of Greece to better characterise the bioavailable Sr isotope composition of the Greek surface environment and to provide future mobility studies with a better understanding of the range in bioavailable  $^{87}\text{Sr}/^{86}\text{Sr}$  values. These were defined as the average bioavailable  $^{87}\text{Sr}/^{86}\text{Sr}$  signature of the region/geology  $\pm$  its double standard deviation ( $\bar{x} \pm 2\sigma$ ) to ensure a broad applicability. The ranges defined herein should be considered as a starting point for future mobility studies and might need to be expanded or redefined based on the goal or target area of these studies.
- 4) Bioavailable  $^{87}\text{Sr}/^{86}\text{Sr}$  isotope baselines were defined for ten of the 13 administrative regions of Greece. The narrowest baselines are calculated for West Greece ( $0.70832 \pm 0.00049$ ;  $\bar{x} \pm 2\sigma$ ;  $n = 17$ ) and Crete ( $0.70888 \pm 0.00054$ ;  $\bar{x} \pm 2\sigma$ ;  $n = 17$ ). Attica, the South Aegean, and Central Greece are characterised by slightly wider, but still unradiogenic baselines of  $0.70859 \pm 0.00066$  ( $\bar{x} \pm 2\sigma$ ;  $n = 10$ ),  $0.70889 \pm 0.00083$  ( $\bar{x} \pm 2\sigma$ ;  $n = 28$ ) and  $0.70862 \pm 0.00092$  ( $\bar{x} \pm 2\sigma$ ;  $n = 42$ ), respectively. Thessaly, Central Macedonia and Athos and the North Aegean are characterised by slightly wider ranges in bioavailable  $^{87}\text{Sr}/^{86}\text{Sr}$  values of the proxies, defining baselines of  $0.70870 \pm 0.00113$  ( $\bar{x} \pm 2\sigma$ ;  $n = 11$ ),  $0.70960 \pm 0.00122$  ( $\bar{x} \pm 2\sigma$ ;  $n = 12$ ) and  $0.70925 \pm 0.00201$  ( $\bar{x} \pm 2\sigma$ ;  $n = 8$ ), respectively. The widest bioavailable  $^{87}\text{Sr}/^{86}\text{Sr}$  baseline ranges are defined for the Peloponnese and West Macedonia with  $0.70936 \pm 0.00617$  ( $\bar{x} \pm 2\sigma$ ;  $n = 61$ ) and  $0.71033 \pm 0.00780$  ( $\bar{x} \pm 2\sigma$ ;  $n = 8$ ), respectively. This likely reflects the wide range of different geological ages represented in the rock outcrops exposed in these regions,

which release highly variable Sr isotope fractions into the biosphere. In Central Greece, the Peloponnese, West Macedonia, Central Macedonia and Athos and West Greece, we measured some outlier-like values with  $^{87}\text{Sr}/^{86}\text{Sr}$  values higher than their respective upper baseline ranges. These values are typically from samples taken from older, Palaeozoic or Precambrian rock outcrops, suggesting that additional sampling in these areas might be necessary to better constrain the range  $^{87}\text{Sr}/^{86}\text{Sr}$  typical for these regions. For the geographical regions of East Macedonia and Thrace, Epirus and the Ionian Islands not enough bioavailable  $^{87}\text{Sr}/^{86}\text{Sr}$  data is published to date to calculate statistically meaningful baselines.

- 5) The five main surface lithology groups of Greece are characterised by very different statistical, bioavailable  $^{87}\text{Sr}/^{86}\text{Sr}$  ranges. Areas with Mesozoic and Cenozoic sediments are characterised by an unradiogenic, narrow Sr isotope range of  $0.70853 \pm 0.00094$  ( $\bar{x} \pm 2\sigma$ ;  $n = 74$ ) and  $0.70866 \pm 0.00103$  ( $\bar{x} \pm 2\sigma$ ;  $n = 92$ ), respectively. The statistical range in bioavailable  $^{87}\text{Sr}/^{86}\text{Sr}$  values for areas characterised by abundant igneous rock outcrops is calculated as  $0.70865 \pm 0.00082$  ( $\bar{x} \pm 2\sigma$ ;  $n = 14$ ). However, it appears that the bioavailable Sr contributions to the surface environment from weathering of igneous rocks plays a minor role in determining the bioavailable  $^{87}\text{Sr}/^{86}\text{Sr}$  signatures of Greece. Should this be the case, then future studies should use the Sr isotope ranges typical for adjacent surface lithologies when investigating mobility in areas characterised by igneous outcrops. The calculated bioavailable  $^{87}\text{Sr}/^{86}\text{Sr}$  ranges for samples from areas with Palaeozoic ( $0.71092 \pm 0.00826$ ;  $\bar{x} \pm 2\sigma$ ;  $n = 28$ ) and Precambrian ( $0.71003 \pm 0.00582$ ;  $\bar{x} \pm 2\sigma$ ;  $n = 14$ ) outcrops are statistically wide. This is likely due to a heterogeneous  $^{87}\text{Sr}/^{86}\text{Sr}$  release from the rocks and soils developed on these outcrops, which are expected to be characterised by more radiogenic  $^{87}\text{Sr}/^{86}\text{Sr}$  values. These wide bioavailable  $^{87}\text{Sr}/^{86}\text{Sr}$  signature ranges defined by samples collected in areas with Palaeozoic and Precambrian rock outcrops render geographical provenancing more difficult as they completely overlap with the  $^{87}\text{Sr}/^{86}\text{Sr}$  ranges typical for samples from the other surface lithologies.
- 6) A comparison of the soil leachate  $^{87}\text{Sr}/^{86}\text{Sr}$  values from the cultural layers of Kirrha and Ayios Vasileios with our calculated baselines reveal that these fit well with their respective geographical and geological baselines. This is true when defining the baseline as the average  $^{87}\text{Sr}/^{86}\text{Sr}$  value  $\pm$  the single standard deviation ( $\sigma$ ) and double standard deviation ( $2\sigma$ ), supporting the applicability of our calculated baselines for investigating past human mobility. However, the different  $^{87}\text{Sr}/^{86}\text{Sr}$  baselines show varying degrees of overlap in their respective  $^{87}\text{Sr}/^{86}\text{Sr}$  ranges, which limits their applicability when investigating interregional movement within Greece.

#### CRediT authorship contribution statement

**Anja B. Frank:** Investigation, Formal analysis, Data curation, Writing – original draft. **Robert Frei:** Writing – review & editing. **Ioanna Moutafi:** Writing – review & editing. **Sofia Voutsaki:** Writing – review & editing. **Raphaël Orgeolet:** Writing – review & editing. **Kristian Kristiansen:** Funding acquisition, Writing – review & editing. **Karin M. Frei:** Funding acquisition, Supervision, Writing – review & editing.

#### Declaration of competing interest

The authors declare that they have no known competing financial interests or personal relationships that could have appeared to influence the work reported in this paper.

#### Acknowledgment

The authors want to thank Christina Koureta for her help in the field, Christina Jensen for her assistance in the lab and Toby Leeper for the TIMS support. This research was made possible through the support of the Swedish Foundation for Humanities and Social Sciences grant

M16-0455:1 to KK and of the Carlsberg Foundation “Semper Ardens” research grant CF18-0005 to KMF, which we are very grateful for.

#### Appendix A. Supplementary data

Supplementary data to this article can be found online at <https://doi.org/10.1016/j.scitotenv.2021.148156>.

#### References

- Barton, M., Salters, V.J.M., Huijsmans, J.P.P., 1983. Sr isotope and trace element evidence for the role of continental crust in calc-alkaline volcanism on Santorini and Milos, Aegean Sea, Greece. *Earth Planet. Sci. Lett.* 63, 273–291. [https://doi.org/10.1016/0012-821X\(83\)90042-0](https://doi.org/10.1016/0012-821X(83)90042-0).
- Bentley, R.A., 2006. Strontium isotopes from the earth to the archaeological skeleton: a review. *J. Archaeol. Method Theory* 13, 135–187. <https://doi.org/10.1007/s10816-006-9009-x>.
- BGR, 2020. Geoviewer [WWW Document]. URL [https://geoviewer.bgr.de/mapapps4/resources/apps/geoviewer/index.html?lang=de&tab=geologie&cover=geologie\\_europa&layers=geologie\\_igme5000\\_ags](https://geoviewer.bgr.de/mapapps4/resources/apps/geoviewer/index.html?lang=de&tab=geologie&cover=geologie_europa&layers=geologie_igme5000_ags). (Accessed 7 July 2020).
- Bishop, K.G., Garvie-Lok, S., Haagsma, M., MacKinnon, M., Karapanou, S., 2020. Mobile animal management in the Mediterranean: investigating Hellenistic (323–31 BCE) husbandry practices in Thessaly, Greece using  $\delta^{13}\text{C}$ ,  $\delta^{18}\text{O}$ , and  $^{87}\text{Sr}/^{86}\text{Sr}$  recorded from sheep and goat tooth enamel. *J. Archaeol. Sci. Rep.* 31, 102331. <https://doi.org/10.1016/j.jasrep.2020.102331>.
- Brilli, M., Cavazzini, G., Turi, B., 2005. New data of  $^{87}\text{Sr}/^{86}\text{Sr}$  ratio in classical marble: an initial database for marble provenance determination. *J. Archaeol. Sci.* 32, 1543–1551. <https://doi.org/10.1016/j.jas.2005.04.007>.
- Burke, W.H., Denison, R.E., Hetherington, E.A., Koepnick, R.B., Nelson, H.F., Otto, J.B., 1982. Variation of seawater  $^{87}\text{Sr}/^{86}\text{Sr}$  throughout Phanerozoic time. *Geology* 10, 516–519. [https://doi.org/10.1130/0091-7613\(1982\)10<516:VOSSTP>2.0.CO;2](https://doi.org/10.1130/0091-7613(1982)10<516:VOSSTP>2.0.CO;2).
- Capo, R.C., Stewart, B.W., Chadwick, O.A., 1998. Strontium isotopes as tracers of ecosystem processes: theory and methods. *Geoderma* 82, 197–225. [https://doi.org/10.1016/S0016-7061\(97\)00102-X](https://doi.org/10.1016/S0016-7061(97)00102-X).
- Cavazzuti, C., Skeates, R., Millard, A.R., Nowell, G., Peterkin, J., Bernabò Brea, M., Cardarelli, A., Salzani, L., 2019. Flows of people in villages and large centres in Bronze Age Italy through strontium and oxygen isotopes. *PLoS ONE* 14, e0209693. <https://doi.org/10.1371/journal.pone.0209693>.
- Coelho, I., Castanheira, I., Bordado, J.M., Donard, O., Silva, J.A.L., 2017. Recent developments and trends in the application of strontium and its isotopes in biological related fields. *TrAC Trends Anal. Chem.* C, 45–61. <https://doi.org/10.1016/j.trac.2017.02.005>.
- EGDI, 2019. Map viewer [WWW Document]. URL <http://www.europe-geology.eu/mapviewer/>. (Accessed 13 June 2019).
- Frei, Y., Torrent, J., 2010. Contribution of Saharan dust to Mediterranean soils assessed by sequential extraction and Pb and Sr isotopes. *Chem. Geol.* 275, 19–25. <https://doi.org/10.1016/j.chemgeo.2010.04.007>.
- Evans, J.A., Tatham, S., 2004. Defining ‘local signature’ in terms of Sr isotope composition using a tenth- to twelfth-century Anglo-Saxon population living on a Jurassic clay-carbonate terrain, Rutland, UK. *Geol. Soc. Lond. Spec. Publ.* 232, 237–248. <https://doi.org/10.1144/GSL.SP.2004.232.01.21>.
- Evans, J.A., Montgomery, J., Wildman, G., Boulton, N., 2010. Spatial variations in biosphere  $^{87}\text{Sr}/^{86}\text{Sr}$  in Britain. *J. Geol. Soc.* 167, 1–4. <https://doi.org/10.1144/0016-76492009-090>.
- Flockhart, D.T.T., Kyser, T.K., Chipley, D., Miller, N.G., Norris, D.R., 2015. Experimental evidence shows no fractionation of strontium isotopes ( $^{87}\text{Sr}/^{86}\text{Sr}$ ) among soil, plants, and herbivores: implications for tracking wildlife and forensic science. *Isot. Environ. Health Stud.* 51, 372–381. <https://doi.org/10.1080/10256016.2015.1021345>.
- Frank, A.B., Frei, R., Triantaphyllou, M., Vassilakis, E., Kristiansen, K., Frei, K.M., 2021. Isotopic range of bioavailable strontium on the Peloponnese peninsula, Greece: a multiproxy approach. *Sci. Total Environ.* 774, 145181. <https://doi.org/10.1016/j.scitotenv.2021.145181>.
- Frei, K.M., Frei, R., 2011. The geographic distribution of strontium isotopes in Danish surface waters – a base for provenance studies in archaeology, hydrology and agriculture. *Appl. Geochem.* 26, 326–340. <https://doi.org/10.1016/j.apgeochem.2010.12.006>.
- Frei, R., Frei, K.M., 2013. The geographic distribution of Sr isotopes from surface waters and soil extracts over the island of Bornholm (Denmark) – a base for provenance studies in archaeology and agriculture. *Appl. Geochem.* 38, 147–160. <https://doi.org/10.1016/j.apgeochem.2013.09.007>.
- Frei, K.M., Mannering, U., Kristiansen, K., Allentoft, M.E., Wilson, A.S., Skals, I., Tridico, S., Louise Nosch, M., Willerslev, E., Clarke, L., Frei, R., 2015. Tracing the dynamic life story of a Bronze Age Female. *Sci. Rep.* 5, 10431. <https://doi.org/10.1038/srep10431>.
- Frei, R., Frei, K.M., Kristiansen, S.M., Jessen, S., Schullehner, J., Hansen, B., 2020. The link between surface water and groundwater-based drinking water – strontium isotope spatial distribution patterns and their relationships to Danish sediments. *Appl. Geochem.*, 104698. <https://doi.org/10.1016/j.apgeochem.2020.104698>.
- Gale, N.H., Einfalt, H.C., Hubberten, H.W., Jones, R.E., 1988. The sources of Mycenaean gypsum. *J. Archaeol. Sci.* 15, 57–72. [https://doi.org/10.1016/0305-4403\(88\)90019-2](https://doi.org/10.1016/0305-4403(88)90019-2).
- Gärtner, C., Bröcker, M., Strauss, H., Farber, K., 2011. Strontium-, carbon- and oxygen-isotope compositions of marbles from the Cycladic blueschist belt, Greece. *Geol. Mag.* 148, 511–528. <https://doi.org/10.1017/S001675681100001X>.
- Goudie, A.S., Middleton, N.J., 2001. Saharan dust storms: nature and consequences. *Earth-Sci. Rev.* 56, 179–204. [https://doi.org/10.1016/S0012-8252\(01\)00067-8](https://doi.org/10.1016/S0012-8252(01)00067-8).



- Grimstead, D.N., Nugent, S., Whipple, J., 2017. Why a standardization of strontium isotope baseline environmental data is needed and recommendations for methodology. *Adv. Archaeol. Pract.* 5, 184–195. <https://doi.org/10.1017/aap.2017.6>.
- Grousset, F.E., Biscaye, P.E., 2005. Tracing dust sources and transport patterns using Sr, Nd and Pb isotopes. *Chem. Geol.* 222, 149–167. <https://doi.org/10.1016/j.chemgeo.2005.05.006>.
- Grousset, F.E., Parra, M., Bory, A., Martinez, P., Bertrand, P., Shimmield, G., Ellam, R.M., 1998. Saharan wind regimes traced by the Sr–Nd isotopic composition of subtropical atlantic sediments: last glacial maximum vs today. *Quat. Sci. Rev.* 17, 395–409. [https://doi.org/10.1016/S0277-3791\(97\)00048-6](https://doi.org/10.1016/S0277-3791(97)00048-6).
- Hoogewerff, J.A., Reimann, Clemens, Ueckermann, H., Frei, R., Frei, K.M., van Aswegen, T., Stirling, C., Reid, M., Clayton, A., Ladenberger, A., Albanese, S., Andersson, M., Baritz, R., Batista, M.J., Bel-lan, A., Birke, M., Cicchella, D., Demetriades, A., De Vivo, B., De Vos, W., Dinelli, E., Đuriš, M., Dusza-Dobek, A., Eggen, O.A., Eklund, M., Ernstsen, V., Filzmoser, P., Flight, D.M.A., Forrester, S., Fuchs, M., Fügedi, U., Gilucis, A., Gregorauskiene, V., De Groot, W., Gulan, A., Halamić, J., Haslinger, E., Hayoz, P., Hoffmann, R., Hrvatovic, H., Husnjak, S., Janik, L., Jordan, G., Kaminari, M., Kirby, J., Kivisilla, J., Klos, V., Krone, F., Kwečko, F., Kutl, L., Lima, A., Locutura, J., Lucivjansky, D.P., Mann, A., Mackovych, D., Matschullat, J., McLaughlin, M., Malyuk, B.J., Maquill, R., Meuli, R.G., Mol, G., Negrel, P., Connor, O., Oorts, R.K., Ottesen, R.T., Pasieczna, A., Petersell, W., Pfeleiderer, S., Poňavič, M., Pramuka, S., Prazeres, C., Rauch, U., Radusinović, S., Reimann, C., Sadeghi, M., Salpeteur, I., Scanlon, R., Schedl, A., Scheib, A.J., Schoeters, I., Šečič, P., Sellersjö, E., Skopljak, F., Slaninka, I., Soriano-Disla, J.M., Šorša, A., Srvkota, R., Stafliov, T., Tarvainen, T., Trendavilov, V., Valera, P., Verougstraete, V., Vidojević, D., Zissimos, A., Zomeni, Z., 2019. Bioavailable 87Sr/86Sr in European soils: a baseline for provenancing studies. *Sci. Total Environ.* 672, 1033–1044. <https://doi.org/10.1016/j.scitotenv.2019.03.387>.
- Hosono, T., Nakano, T., Igeta, A., Tayasu, I., Tanaka, T., Yachi, S., 2007. Impact of fertilizer on a small watershed of Lake Biwa: use of sulfur and strontium isotopes in environmental diagnosis. *Sci. Total Environ.* 384, 342–354. <https://doi.org/10.1016/j.scitotenv.2007.05.033>.
- Ladegaard-Pedersen, P., Achilleos, M., Dörflinger, G., Frei, R., Kristiansen, K., Frei, K.M., 2019. A strontium isotope baseline of Cyprus. Assessing the use of soil leachates, plants, groundwater and surface water as proxies for the local range of bioavailable strontium isotope composition. *Sci. Total Environ.*, 134714 <https://doi.org/10.1016/j.scitotenv.2019.134714>.
- Ladegaard-Pedersen, P., Sabatini, S., Frei, R., Kristiansen, K., Frei, K.M., 2021. Testing Late Bronze Age mobility in southern Sweden in the light of a new multi-proxy strontium isotope baseline of Scania. *PLoS ONE* 16, e0250279. <https://doi.org/10.1371/journal.pone.0250279>.
- Lagia, A., Moutafi, I., Orgeoleot, R., Skorda, D., Zurbach, J., 2016. Revisiting the tomb: mortuary practices in habitation areas in the transition to the Late Bronze Age at Kirra, Phocis. *Staging Death: Funerary Performance, Architecture and Landscape in the Aegean*. De Gruyter, Berlin, pp. 206–232.
- Leslie, B.G., 2012. Residential Mobility in the Rural Greek Past: A Strontium Isotope Investigation. (MA Thesis). University of Alberta, Edmonton, Canada.
- Liu, W.-J., Liu, C.-Q., Zhao, Z.-Q., Xu, Z.-F., Liang, C.-S., Li, L., Feng, J.-Y., 2013. Elemental and strontium isotopic geochemistry of the soil profiles developed on limestone and sandstone in karstic terrain on Yunnan-Guizhou Plateau, China: implications for chemical weathering and parent materials. *J. Asian Earth Sci.* 67–68, 138–152. <https://doi.org/10.1016/j.jseas.2013.02.017>.
- Liu, W., Jiang, H., Shi, C., Zhao, T., Liang, C., Hu, J., Xu, Z., 2016. Chemical and strontium isotopic characteristics of the rivers around the Badain Jaran Desert, northwest China: implication of river solute origin and chemical weathering. *Environ. Earth Sci.* 75, 1119. <https://doi.org/10.1007/s12665-016-5910-0>.
- Maurer, A.-F., Galer, S.J.G., Knipper, C., Beierlein, L., Nunn, E.V., Peters, D., Tütken, T., Alt, K.W., Schöne, B.R., 2012. Bioavailable 87Sr/86Sr in different environmental samples – effects of anthropogenic contamination and implications for isoscapes in past migration studies. *Sci. Total Environ.* 433, 216–229. <https://doi.org/10.1016/j.scitotenv.2012.06.046>.
- McArthur, J.M., Howarth, R.J., Bailey, T.R., 2001. Strontium isotope stratigraphy: LOWESS version 3: best fit to the marine Sr–Nd isotope curve for 0–509 Ma and accompanying look-up table for deriving numerical age. *J. Geol.* 109, 155–170. <https://doi.org/10.1086/319243>.
- Montgomery, J., 2010. Passports from the past: investigating human dispersals using strontium isotope analysis of tooth enamel. *Ann. Hum. Biol.* 37, 325–346. <https://doi.org/10.3109/03014461003649297>.
- Moutafi, I., Voutsaki, S., 2016. Commingled burials and shifting notions of the self at the onset of the Mycenaean era (1700–1500 BCE): the case of the Ayios Vasiliou North Cemetery, Laconia. *J. Archaeol. Sci. Rep.* 10, 780–790. <https://doi.org/10.1016/j.jasrep.2016.05.037>.
- Nafplioti, A., 2008. “Mycenaean” political domination of Knossos following the Late Minoan IB destructions on Crete: negative evidence from strontium isotope ratio analysis (87Sr/86Sr). *J. Archaeol. Sci.* 35, 2307–2317. <https://doi.org/10.1016/j.jas.2008.03.006>.
- Nafplioti, A., 2011. Tracing population mobility in the Aegean using isotope geochemistry: a first map of local biologically available 87Sr/86Sr signatures. *J. Archaeol. Sci.* 38, 1560–1570. <https://doi.org/10.1016/j.jas.2011.02.021>.
- Nakano, T., Yokoo, Y., Yamanaka, M., 2001. Strontium isotope constraint on the provenance of basic cations in soil water and stream water in the Kawakami volcanic watershed, central Japan. *Hydrol. Process.* 15, 1859–1875. <https://doi.org/10.1002/hyp.244>.
- Panagiotopoulou, E., Montgomery, J., Nowell, G., Peterkin, J., Doulergi-Intzesiloglou, A., Arachoviti, P., Katakouta, S., Tsiouka, F., 2018. Detecting mobility in early Iron Age Thessaly by strontium isotope analysis. *Eur. J. Archaeol.* 21, 590–611. <https://doi.org/10.1017/eea.2017.88>.
- Papanikolaou, D., 2013. Tectonostratigraphic models of the Alpine terranes and subduction history of the Hellenides. *Tectonophysics* 595–596, 1–24. <https://doi.org/10.1016/j.tecto.2012.08.008>.
- Papanikolaou, D., 2015. ΓΕΩΛΟΓΙΑ ΤΗΣ ΕΛΛΑΔΑΣ. Patakis publications, Athens.
- Pawlewicz, M.J., Steinsouer, D.W., Gautier, D.L., 1997. Map Showing Geology, Oil and Gas Fields, and Geologic Provinces of Europe Including Turkey (Report No. 97-4701), Open-File Report. Reston, VA. <https://doi.org/10.3133/ofr974701>.
- Prevedorou, E.A., 2015. The Role of Kin Relations and Residential Mobility During the Transition From Final Neolithic to Early Bronze Age in Attica, Greece. Arizona State University, Phoenix, AZ.
- Price, T.D., Burton, J.H., Bentley, R.A., 2002. The characterization of biologically available strontium isotope ratios for the study of prehistoric migration. *Archaeometry* 44, 117–135. <https://doi.org/10.1111/1475-4754.00047>.
- Richards, M., Harvati, K., Grimes, V., Smith, C., Smith, T., Hublin, J.-J., Karkanas, P., Panagiotopoulou, E., 2008. Strontium isotope evidence of Neanderthal mobility at the site of Lakonis, Greece using laser-ablation PIMMS. *J. Archaeol. Sci.* 35, 1251–1256. <https://doi.org/10.1016/j.jas.2007.08.018>.
- Rose, M., Baxter, M., Brereton, N., Baskaran, C., 2010. Dietary exposure to metals and other elements in the 2006 UK Total Diet Study and some trends over the last 30 years. *Food Addit. Contam. Part Chem. Anal. Control Expo. Risk Assess.* 27, 1380–1404. <https://doi.org/10.1080/19440049.2010.496794>.
- Ryan, S.E., Snoeck, C., Crowley, Q.G., Babechuk, M.G., 2018. 87Sr/86Sr and trace element mapping of geosphere-hydrosphere-biosphere interactions: a case study in Ireland. *Appl. Geochem.* 92, 209–224. <https://doi.org/10.1016/j.apgeochem.2018.01.007>.
- Thirlwall, M.F., 1991. Long-term reproducibility of multicollector Sr and Nd isotope ratio analysis. *Chem. Geol.* 94, 85–104. [https://doi.org/10.1016/S0009-2541\(10\)80021-X](https://doi.org/10.1016/S0009-2541(10)80021-X).
- Tommasini, S., Marchionni, S., Tescione, I., Casalini, M., Braschi, E., Avanzinelli, R., Conticelli, S., 2018. Strontium isotopes in biological material: a key tool for the geographic traceability of foods and humans beings. In: Gupta, D.K., Walther, C. (Eds.), *Behaviour of Strontium in Plants and the Environment*. Springer International Publishing, Cham, pp. 145–166. [https://doi.org/10.1007/978-3-319-66574-0\\_10](https://doi.org/10.1007/978-3-319-66574-0_10).
- Tremba, E.L., Faure, G., Katsikatsos, G.C., Summerson, C.H., 1975. Strontium-isotope composition in the Thethys Sea, Euboea, Greece. *Chem. Geol.* 16, 109–120. [https://doi.org/10.1016/0009-2541\(75\)90003-0](https://doi.org/10.1016/0009-2541(75)90003-0).
- Triantaphyllou, S., Nikita, E., Kador, T., 2015. Exploring mobility patterns and biological affinities in the Southern Aegean: first insights from Early Bronze Age Eastern Crete. *Ann. Br. Sch. Athens* 110, 3–25. <https://doi.org/10.1017/S0068245415000064>.
- Tukey, J.W., 1977. *Exploratory Data Analysis*. Addison-Wesley Series in Behavioral Science. Quantitative Methods. Addison-Wesley, Reading, MA, US.
- Vaiglova, P., Halstead, P., Pappa, M., Triantaphyllou, S., Valamoti, S.M., Evans, J., Fraser, R., Karkanas, P., Kay, A., Lee-Thorp, J., Bogaard, A., 2018. Of cattle and feasts: multi-isotope investigation of animal husbandry and communal feasting at Neolithic Makriyalos, northern Greece. *PLoS ONE* 13, e0194474. <https://doi.org/10.1371/journal.pone.0194474>.
- Valsami-Jones, E., Cann, J.R., 1994. Controls on the Sr and Nd isotopic compositions of hydrothermally altered rocks from the Pindos Ophiolite, Greece. *Earth Planet. Sci. Lett.* 125, 39–54. [https://doi.org/10.1016/0012-821X\(94\)90205-4](https://doi.org/10.1016/0012-821X(94)90205-4).
- Vasilatou, V., Manousakas, M., Gini, M., Diapouli, E., Scoullou, M., Eleftheriadis, K., 2017. Long term flux of Saharan dust to the Aegean Sea around the Attica Region, Greece. *Front. Mar. Sci.* 4. <https://doi.org/10.3389/fmars.2017.00042>.
- Voerkelius, S., Lorenz, G.D., Rummel, S., Quélet, C.R., Heiss, G., Baxter, M., Brach-Papa, C., Deters-Iltzberger, P., Hoelzl, S., Hoogewerff, J., Ponzevera, E., Van Bocxstaele, M., Ueckermann, H., 2010. Strontium isotopic signatures of natural mineral waters, the reference to a simple geological map and its potential for authentication of food. *Food Chem.* 118, 933–940. <https://doi.org/10.1016/j.foodchem.2009.04.125>.
- Wang, X., Zhang, X., Fan, A., Sampson, A., Wu, X., Gao, J., Huang, F., Jin, Z., 2019. Strontium isotopic evidence for the provenance of occupants and subsistence of Sarakenos Cave in prehistoric Greece. *Quat. Int.* 508, 13–22. <https://doi.org/10.1016/j.quaint.2018.10.009>.
- Whelton, H.L., Lewis, J., Halstead, P., Isaakidou, V., Triantaphyllou, S., Tzevelekidi, V., Kotsakis, K., Evershed, R.P., 2018. Strontium isotope evidence for human mobility in the Neolithic of northern Greece. *J. Archaeol. Sci. Rep.* 20, 768–774. <https://doi.org/10.1016/j.jasrep.2018.06.020>.
- Whipkey, C.E., Capo, R.C., Chadwick, O.A., Stewart, B.W., 2000. The importance of sea spray to the cation budget of a coastal Hawaiian soil: a strontium isotope approach. *Chem. Geol.* 168, 37–48. [https://doi.org/10.1016/S0009-2541\(00\)00187-X](https://doi.org/10.1016/S0009-2541(00)00187-X).
- Zhang, X., Xu, Z., Liu, W., Moon, S., Zhao, T., Zhou, X., Zhang, J., Wu, Y., Jiang, H., Zhou, L., 2019. Hydro-geochemical and Sr isotope characteristics of the Yalong River Basin, Eastern Tibetan Plateau: implications for chemical weathering and controlling factors. *Geochem. Geophys. Geosyst.* 20, 1221–1239. <https://doi.org/10.1029/2018GC007769>.
- Zieliński, M., Dopierała, J., Belka, Z., Walczak, A., Siewpak, M., Jakubowicz, M., 2016. Sr isotope tracing of multiple water sources in a complex river system, Noteć River, central Poland. *Sci. Total Environ.* 548–549, 307–316. <https://doi.org/10.1016/j.scitotenv.2016.01.036>.